




# Resource Optimisation of Coherently Controlled Quantum Computations with the PBS-calculus

Alexandre Clément   

Université de Lorraine, CNRS, Inria, LORIA, F-54000 Nancy, France

Simon Perdrix   

Université de Lorraine, CNRS, Inria, LORIA, F-54000 Nancy, France

---

## Abstract

Coherent control of quantum computations can be used to improve some quantum protocols and algorithms. For instance, the complexity of implementing the permutation of some given unitary transformations can be strictly decreased by allowing coherent control, rather than using the standard quantum circuit model. In this paper, we address the problem of optimising the resources of coherently controlled quantum computations. We refine the PBS-calculus, a graphical language for coherent control which is inspired by quantum optics. In order to obtain a more resource-sensitive language, it manipulates abstract gates – that can be interpreted as queries to an oracle – and more importantly, it avoids the representation of useless wires by allowing unsaturated polarising beam splitters. Technically the language forms a coloured prop. The language is equipped with an equational theory that we show to be sound, complete, and minimal.

Regarding resource optimisation, we introduce an efficient procedure to minimise the number of oracle queries of a given diagram. We also consider the problem of minimising both the number of oracle queries and the number of polarising beam splitters. We show that this optimisation problem is NP-hard in general, but introduce an efficient heuristic that produces optimal diagrams when at most one query to each oracle is required.

**2012 ACM Subject Classification** Theory of computation → Quantum computation theory; Theory of computation → Axiomatic semantics; Theory of computation → Categorical semantics

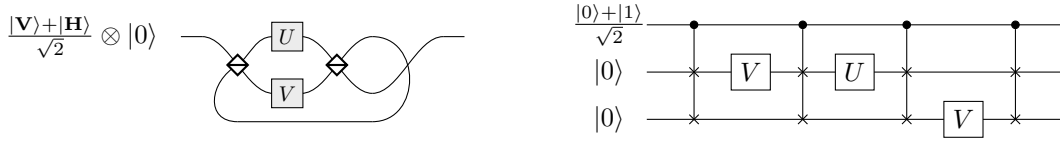
**Keywords and phrases** Quantum computing, Graphical language, Coherent control, Completeness, Resource optimisation, NP-hardness

**Funding** This work is funded by ANR-17-CE25-0009 SoftQPro, ANR-17-CE24-0035 VanQuTe, PIA-GDN/Quantex, and LUE / UOQ, the PEPR integrated project EPiQ ANR-22-PETQ-0007 part of Plan France 2030, and by “*Investissements d’avenir*” (ANR-15-IDEX-02) program of the French National Research Agency; the European Project NExt ApplicationS of Quantum Computing (NEASQC), funded by Horizon 2020 Program inside the call H2020-FETFLAG-2020-01 (Grant Agreement 951821), and the HPCQS European High-Performance Computing Joint Undertaking (JU) under grant agreement No 101018180.

## 1 Introduction

Most models of quantum computation (like quantum circuits) and most quantum programming languages are based on the *quantum data/classical control* paradigm. In other words, based on a set of quantum primitives (e.g. unitary transformations, quantum measurements), the way these primitives are applied on a register of qubits is either fixed or classically controlled.

However, quantum mechanics offers more general control of operations: for instance in quantum optics it is easy to control the trajectory of a system, like a photon, based on its polarisation using a *polarising beam splitter*. One can then position distinct quantum primitives on the distinct trajectories. Since the polarisation of a photon can be in superposition, it achieves some form of quantum control, called coherent control: the quantum primitives are applied in superposition depending on the state of another quantum system. Coherent



■ **Figure 1** [Left] Coherently controlled quantum computation for solving the commuting problem. Only two queries are used: one query to  $U$  and one query to  $V$ . [Right] Optimal circuit for solving the commuting problem, where the 3-qubit gate is a control-swap. Notice that three queries are necessary in the quantum circuit model.

control is not only a subject of interest for foundations of quantum mechanics [24, 31, 38], it also leads to advantages in solving computational problems [19, 5, 15, 32] and in designing more efficient protocols [20, 10, 1, 18, 23].

Indeed, some problems can be solved more efficiently by using coherent control rather than the usual quantum circuits. This separation has been proved in a multi-oracle model where the measure of complexity is the number of queries to (a single or several distinct) oracles, which are generally unitary maps. The simplest example is the following problem [10]: given two oracles  $U$  and  $V$  with the promise that they are either commuting or anti-commuting, decide whether  $U$  and  $V$  are commuting or not. This problem can be solved using the so-called quantum switch [11] which can be implemented using only two queries by means of coherent control, whereas solving this problem requires at least 3 queries (e.g. two queries to  $U$  and one query to  $V$ ) in the quantum circuit model (see Figure 1).

In this paper, we address the problem of optimising resources of coherently controlled quantum computations. To do so, we first refine the framework of the PBS-calculus – a graphical language for coherently controlled quantum computation – to make it more resource-sensitive. Then, we consider the problem of optimising the number of queries, and also the number of polarising beam splitters, of a given coherently controlled quantum computation, described as a PBS-diagram.

**PBS-calculus.** The PBS-calculus is a graphical language that has been introduced [13] to represent and reason about quantum computations involving coherent control of quantum operations. Inspired by quantum optics [12], the polarising beam splitter (PBS for short), denoted  $\bowtie$  is at the heart of the language: when a photon enters the PBS, say from the top left, it is reflected (and hence outputted on the top right) if its polarisation is vertical; or transmitted (and hence outputted on the bottom right) if its polarisation is horizontal. If the polarisation is a superposition of vertical and horizontal, the photon is outputted in a superposition of two positions. As a consequence, the trajectory of a particle, say a photon, will depend on its polarisation. The second main ingredient of the PBS-calculus are the gates, denoted  $\boxed{U}$  which applies some transformation  $U$  on a data register. Notice that the gates never act on the polarisation of the particle.

PBS-diagrams, which form a traced symmetric monoidal category (more precisely a traced prop [28]), are equipped with an equational theory that allows one to transform a diagram. The equational theory has been proved to be sound, complete, and minimal [13].

Notice that a PBS-diagram may have some useless wires, like in the example of the “half quantum switch”, see Figure 2 (left). We refine the PBS-calculus in order to allow one to remove these useless wires, leading to unsaturated PBS (or 3-leg PBS) like  $\overline{\bowtie}$  or  $\underline{\bowtie}$ . To avoid ill-formed diagrams like  $\overline{\bowtie}\underline{\bowtie}$ , a typing discipline is necessary. To this end, we use the framework of coloured props: each wire has 3 possible colours: black, red and blue which can be interpreted as follows: a photon going through a blue (resp. red) wire



■ **Figure 2** A coherent control of  $U$  and  $V$ , also called a half quantum switch: when the initial polarisation is vertical ( $\mathbf{V}$ ),  $U$  is applied on the data register, when the polarisation is horizontal ( $\mathbf{H}$ ),  $V$  is applied. Whatever the polarisation is, the particle always goes out of the top port of the second beam splitter. On the right-hand side the diagram is made of beam splitters with a missing leg, whereas on the left-hand side standard beam splitters are used, and a useless trace is added.

must have a horizontal (resp. vertical) polarisation.

The introduction of unsaturated polarising beam splitters requires to revisit the equational theory of the PBS-calculus. The heart of the refined equational theory is the axiomatisation of the 3-leg polarising beam splitters, together with some additional equations which govern how 4-leg polarising beam splitters can be decomposed into 3-leg ones. To show the completeness of the refined equational theory, we introduce normal forms and show that any diagram can be put in normal form. Finally, we also show the minimality of the equational theory by proving that none of the equations can be derived from the other ones.

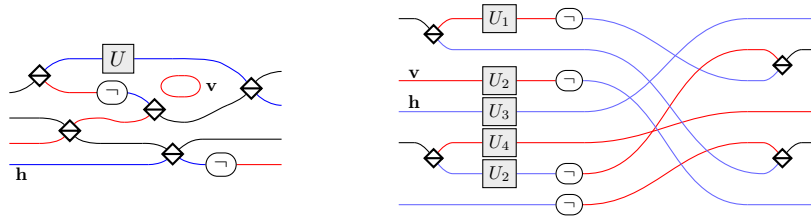
**Resource Optimisation.** The PBS-calculus, thanks to its refined equational theory, provides a way to detect and remove dead-code in a diagram. We exploit this property to address the crucial question of resource optimisation. We introduce a specific form of diagrams that minimises the number of gates, more precisely the number of queries to oracles, with an appropriate modelisation of oracles. We provide an efficient procedure to transform any diagram into this specific form. We then focus on the problem of optimising both the number of queries and the number of polarising beam splitters. We refine the previous procedure, leading to an efficient heuristic. We show that the produced diagrams are optimal when every oracle is queried at most once, but might not be optimal in general. We actually show that the general optimisation problem is NP-hard using a reduction from the *maximum Eulerian cycle decomposition problem* [9].

**Related work.** Several languages have been designed to represent coherently controlled quantum computation: some of them are extensions of quantum circuits, and other diagrammatic languages [35, 6, 36, 34]; others are based on abstract programming languages [2, 37, 17, 16, 7]. While there are numerous works on resource-optimisation of quantum computation, in particular for quantum circuits [27, 4, 30], there was, up to our knowledge, no procedure for resource optimisation of coherently controlled quantum computation.

## 2 Coloured PBS-Diagrams

We use the formalism of traced coloured props (i.e. small traced symmetric strict monoidal categories whose objects are freely spanned by the elements of a set of colours) to represent coherently controlled quantum computations. We are going to use the “colours”  $\mathbf{v}$ ,  $\mathbf{h}$ ,  $\top$ , to denote respectively vertical, horizontal or possibly both polarisations.

► **Definition 1.** Given a monoid  $M$ , let  $\mathbf{Diag}^M$  be the traced coloured prop with colours  $\{\mathbf{v}, \mathbf{h}, \top\}$  freely generated by the following generators, for any  $U \in M$ :



■ **Figure 3** (Left) An example of diagram of type  $\top \oplus \top \oplus \mathbf{v} \oplus \mathbf{h} \rightarrow \top \oplus \mathbf{h} \oplus \top \oplus \mathbf{v}$ . (Right) An example of a diagram of type  $\top \oplus \mathbf{v} \oplus \mathbf{h} \oplus \top \oplus \mathbf{h} \rightarrow \mathbf{h} \oplus \top \oplus \mathbf{v} \oplus \top \oplus \mathbf{h}$ , in a particular form that we will call *normal form* (see Definition 15).

	$\top \oplus \top \rightarrow \top \oplus \top$		$\top \oplus \mathbf{v} \rightarrow \mathbf{v} \oplus \top$		$\top \rightarrow \mathbf{h} \oplus \mathbf{v}$
	$\mathbf{h} \oplus \top \rightarrow \mathbf{h} \oplus \top$		$\mathbf{v} \oplus \top \rightarrow \top \oplus \mathbf{v}$		$\mathbf{v} \oplus \mathbf{h} \rightarrow \top$
	$\top \oplus \mathbf{h} \rightarrow \top \oplus \mathbf{h}$		$\top \rightarrow \mathbf{v} \oplus \mathbf{h}$		$\mathbf{h} \oplus \mathbf{v} \rightarrow \top$
	$\top \rightarrow \top$		$\mathbf{v} \rightarrow \mathbf{h}$		$\mathbf{h} \rightarrow \mathbf{v}$
	$\top \rightarrow \top$		$\mathbf{v} \rightarrow \mathbf{v}$		$\mathbf{h} \rightarrow \mathbf{h}$

The morphisms of  $\mathbf{Diag}^M$  are called M-diagrams or simply diagrams when M is irrelevant or clear from the context. Intuitively, the diagrams are inductively obtained by composition of the generators from Definition 1 using the sequential composition  $D_2 \circ D_1$ , the parallel composition  $D_3 \oplus D_4$ , and the trace  $Tr_d(D)$  which are respectively depicted as

follows:  $\begin{array}{c} \boxed{D_1} \\ \vdots \\ \boxed{D_2} \end{array} \quad \begin{array}{c} \boxed{D_3} \\ \vdots \\ \boxed{D_4} \end{array} \quad \begin{array}{c} \boxed{D} \\ \vdots \\ \boxed{D} \end{array} \quad \text{with a trace symbol } \text{Tr}_d$ . Notice that these compositions should type-check,

i.e.  $D_1 : a \rightarrow b$ ,  $D_2 : b \rightarrow c$  and  $D : a \oplus d \rightarrow b \oplus d$  with  $d \in \{\top, \mathbf{v}, \mathbf{h}\}$ . The axioms of the traced coloured prop guarantee that the diagrams are defined up to deformation: two diagrams whose graphical representations are isomorphic are equal.

Regarding notations, we use actual colours for wires: blue for  $\mathbf{h}$ -wires, red for  $\mathbf{v}$ -wires, and black for  $\top$ -wires. We also add labels on the wires, which are omitted when clear from the context, so that there is no loss of information in the case of a colour-blind reader or black and white printing.<sup>1</sup> Two examples of diagrams are given in Figure 3.

Unless specified, the unit of M is denoted  $I$  and its composition is  $\cdot$  which will be generally omitted ( $VU$  rather than  $V \cdot U$ ). The main two examples of monoids we consider in the rest of the paper are:

- The monoid  $\mathcal{U}(\mathcal{H})$  of isometries of a Hilbert space  $\mathcal{H}$  with the usual composition. When  $\mathcal{H}$  is of finite dimension, the elements of  $\mathcal{U}(\mathcal{H})$  are unitary maps. With a slight abuse of notations, the corresponding traced coloured prop of diagrams is denoted  $\mathbf{Diag}^{\mathcal{H}}$ .
- The free monoid  $\mathcal{G}^*$  on some set  $\mathcal{G}$ . The gates, when the monoid is freely generated, can be interpreted as queries to oracles (each element of  $\mathcal{G}$  corresponds to an oracle): the gates implement *a priori* arbitrary operations with no particular structures. We use the term *abstract diagram* when the underlying monoid is freely generated, and we refer to the elements of  $\mathcal{G}$  as *names*. Notice that the free monoid case can also be seen as an extension of *bare diagrams* [8].

<sup>1</sup> With the convention that the type  $\top$  is always omitted (in other words, a wire of ambiguous type is black by convention). See [14], Example 1.7 for additional explanations about how to infer the omitted types.

There are other examples of interests: One can consider for instance a monoid of commuting or anticommuting gates, that can be used to model the problem studied in [10]. Another example is the monoid of  $n$ -qubit quantum circuits whose generators are layers of gates acting on  $n$  qubits (e.g.  $H \otimes CNot \otimes I \otimes H$  when  $n = 5$  where  $H$  is the 1-qubit Hadamard gate,  $CNot$  the 2-qubit controlled-not gate, and  $I$  the 1-qubit identity) and whose composition is the sequential composition of circuits. The monoid can be quotiented by equations like  $(H \otimes I) \cdot (I \otimes H) = H \otimes H$  and  $(H \otimes I) \cdot (H \otimes I) = I \otimes I$ . Finally, one can consider the monoid of unitary purifications<sup>2</sup> used to describe coherent control of quantum channels [8].

### 3 Semantics

The input of a diagram is a single particle, which has a polarisation, a position and a data register. A basis state for the polarisation is either vertical or horizontal, and a basis state for the position is an integer which corresponds to the wire on which the particle is located. The type of a diagram restricts the possible input/output configurations: if  $D : \mathbf{v} \oplus \top \rightarrow \mathbf{h} \oplus \mathbf{h} \oplus \mathbf{v}$  then the possible input (resp. output) configurations are the following polarisation-position pairs:  $\{(\mathbf{V}, 0), (\mathbf{V}, 1), (\mathbf{H}, 1)\}$  (resp.  $\{(\mathbf{H}, 0), (\mathbf{H}, 1), (\mathbf{V}, 2)\}$ ). More generally for any object  $a$ , let  $[a]$  be the set of possible configurations, and  $|a|$  be its size, inductively defined as follows:  $|I| = 0$ ,  $|a \oplus \top| = |a \oplus \mathbf{v}| = |a \oplus \mathbf{h}| = |a| + 1$ , and  $[I] = \emptyset$ ,  $[a \oplus \mathbf{v}] = [a] \cup \{(\mathbf{V}, |a|)\}$ ,  $[a \oplus \mathbf{h}] = [a] \cup \{(\mathbf{H}, |a|)\}$  and  $[a \oplus \top] = [a] \cup \{(\mathbf{V}, |a|), (\mathbf{H}, |a|)\}$ .

The semantics of an M-diagram  $D : a \rightarrow b$  is a map  $[a] \rightarrow [b] \times \mathbf{M}$  which associates with an input configuration  $(c, p)$ , an output configuration  $(c', p')$  and a side effect  $U_k \dots U_1 \in \mathbf{M}$  which represents the action applied on a data register of the particle. Thus the semantics of a diagram can be formulated as follows:

► **Definition 2** (Action semantics). *Given an M-diagram  $D : a \rightarrow b$ , let  $\llbracket D \rrbracket : [a] \rightarrow [b] \times \mathbf{M}$  be inductively defined as:  $\forall D_1 : a \rightarrow b, D_2 : b \rightarrow d, D_3 : d \rightarrow e, D_4 : a \oplus f \rightarrow b \oplus f$ , where  $f \in \{\top, \mathbf{v}, \mathbf{h}\}$ :*

$$\begin{aligned}
\llbracket \text{CNOT} \rrbracket &= \begin{cases} (\mathbf{V}, 0) \mapsto ((\mathbf{V}, 0), I) \\ (\mathbf{H}, 0) \mapsto ((\mathbf{H}, 1), I) \end{cases} & \llbracket \text{CNOT} \rrbracket &= \begin{cases} (\mathbf{V}, 0) \mapsto ((\mathbf{V}, 1), I) \\ (\mathbf{H}, 0) \mapsto ((\mathbf{H}, 0), I) \end{cases} \\
\llbracket \text{CNOT} \rrbracket &= \begin{cases} (\mathbf{V}, 0) \mapsto ((\mathbf{V}, 0), I) \\ (\mathbf{H}, 1) \mapsto ((\mathbf{H}, 0), I) \end{cases} & \llbracket \text{CNOT} \rrbracket &= \begin{cases} (\mathbf{V}, 1) \mapsto ((\mathbf{V}, 0), I) \\ (\mathbf{H}, 0) \mapsto ((\mathbf{H}, 0), I) \end{cases} \\
\llbracket \text{CNOT} \rrbracket &= (c, p) \mapsto \begin{cases} ((c, p), I) & \text{if } c = \mathbf{V} \\ ((c, 1 - p), I) & \text{if } c = \mathbf{H} \end{cases} & \llbracket \text{CNOT} \rrbracket &= (c, p) \mapsto ((c, 1 - p), I) \\
\llbracket \text{CNOT} \rrbracket &= (c, 0) \mapsto ((c, 0), I) & \llbracket \text{CNOT} \rrbracket &= \begin{cases} (\mathbf{V}, 0) \mapsto ((\mathbf{H}, 0), I) \\ (\mathbf{H}, 0) \mapsto ((\mathbf{V}, 0), I) \end{cases} \\
\llbracket \text{CNOT} \rrbracket &= (c, 0) \mapsto ((c, 0), U) & \llbracket \text{CNOT} \rrbracket &= (c, p) \mapsto \begin{cases} \llbracket D_1 \rrbracket (c, p) & \text{if } p < |a| \\ S_a(\llbracket D_3 \rrbracket (c, p - |a|)) & \text{otherwise} \end{cases} & \llbracket D_2 \circ D_1 \rrbracket &= \llbracket D_2 \rrbracket \circ \llbracket D_1 \rrbracket
\end{aligned}$$

<sup>2</sup> Given a Hilbert space  $\mathcal{H}$ , the elements of the monoid are triplets  $[U, |\varepsilon\rangle, \mathcal{E}]$  where  $\mathcal{E}$  is a Hilbert space,  $U : \mathcal{H} \otimes \mathcal{E} \rightarrow \mathcal{H} \otimes \mathcal{E}$  is a unitary transformation, and  $|\varepsilon\rangle \in \mathcal{E}$ . The composition is defined as  $[U_2, |\varepsilon_2\rangle, \mathcal{E}_2] \cdot [U_1, |\varepsilon_1\rangle, \mathcal{E}_1] = [(\sigma_{\mathcal{E}_1, \mathcal{H}} \otimes I)(I \otimes U_2)(\sigma_{\mathcal{H}, \mathcal{E}_1} \otimes I)(U_1 \otimes I), |\varepsilon_1\rangle \otimes |\varepsilon_2\rangle, \mathcal{E}_1 \otimes \mathcal{E}_2]$  where  $\sigma_{\mathcal{K}, \mathcal{K}'}$  is the swap between the two Hilbert spaces  $\mathcal{K}, \mathcal{K}'$ .

$$\llbracket \text{Tr}_f(D_4) \rrbracket = (c, p) \mapsto \begin{cases} \llbracket D_4 \rrbracket (c, p) & \text{if } \pi_{\text{pos}}(\llbracket D_4 \rrbracket (c, p)) < |b| \\ \llbracket D_4 \rrbracket \circ S_{a-b}(\llbracket D_4 \rrbracket (c, p)) & \\ \quad \text{if } \pi_{\text{pos}}(\llbracket D_4 \rrbracket \circ S_{a-b}(\llbracket D_4 \rrbracket (c, p))) < |b| \leq \pi_{\text{pos}}(\llbracket D_4 \rrbracket (c, p)) \\ \llbracket D_4 \rrbracket \circ S_{a-b}(\llbracket D_4 \rrbracket \circ S_{a-b}(\llbracket D_4 \rrbracket (c, p))) & \text{otherwise} \end{cases}$$

where the composition is:  $g \circ f(c, p) = ((c', p''), U'U)$  with  $f(c, p) = ((c', p'), U)$  and  $g(c', p') = ((c'', p''), U')$ ;  $\pi_{\text{pos}} : [a] \times \mathbb{M} \rightarrow \mathbb{N} :: ((c, p), U) \mapsto p$  is the projector on the position; and  $S_a : [b] \times \mathbb{M} \rightarrow [a \oplus b] \times \mathbb{M} :: ((c, p), U) \mapsto ((c, p + |a|), U)$  and  $S_{a-b} : [b] \times \mathbb{M} \rightarrow [a] \times \mathbb{M} :: ((c, p), U) \mapsto ((c, p + |a| - |b|), U)$  shift the position.

Given  $D : a \rightarrow b$  and  $(c, p) \in [a]$ , we denote respectively by  $c_{c,p}^D$ ,  $p_{c,p}^D$  and  $U_{c,p}^D$  the polarisation, the position and the element of  $\mathbb{M}$ , such that  $\llbracket D \rrbracket (c, p) = ((c_{c,p}^D, p_{c,p}^D), U_{c,p}^D)$ . In the case where  $\mathbb{M}$  is the free monoid  $\mathcal{G}^*$ , its elements can be seen as words, so we will use the notation  $w_{c,p}^D$  instead of  $U_{c,p}^D$ .

Notice that the semantics of the trace is not defined as a fixed point but as a finite number of unfoldings. Indeed, like for PBS-diagrams, one can show that any wire of a diagram is used at most twice, each time with a distinct polarisation.

► **Proposition 3.**  $\llbracket \cdot \rrbracket$  is well-defined, i.e. the axioms of the traced coloured prop are sound and the semantics of the trace is well-defined.

**Proof.** This can be proved in a similar way as in Appendix B.1.1 of [13] and Appendix B.1 of [8], noting that our action semantics could equivalently be defined as a big-step path semantics similar to those of [13] and [8] (cf. Section 4.2 of [14]). ◀

### 3.1 Quantum Semantics

Any diagram whose underlying monoid consists of linear maps admits a *quantum semantics*, defined as follows:

► **Definition 4** (Quantum semantics). *Given a monoid  $\mathbb{M}$  of linear maps (with the standard composition) on a complex vector space  $\mathcal{V}$ , for any  $\mathbb{M}$ -diagram  $D : a \rightarrow b$  the quantum semantics of  $D$  is the linear map  $V_D : \mathbb{C}^{[a]} \otimes \mathcal{V} \rightarrow \mathbb{C}^{[b]} \otimes \mathcal{V} :: |c, p\rangle \otimes |\varphi\rangle \mapsto |c_{c,p}^D, p_{c,p}^D\rangle \otimes U_{c,p}^D |\varphi\rangle$ .*

The diagrams in  $\mathbf{Diag}^{\mathcal{H}}$  are valid by construction, in the sense that their semantics are valid quantum evolutions:

► **Proposition 5.** *For any  $D \in \mathbf{Diag}^{\mathcal{H}}$ ,  $V_D : \mathbb{C}^{[a]} \otimes \mathcal{H} \rightarrow \mathbb{C}^{[b]} \otimes \mathcal{H}$  is an isometry.*

**Proof.** The proof is given in Appendix A.1. ◀

Note that  $\llbracket D \rrbracket = \llbracket D' \rrbracket$  implies  $V_D = V_{D'}$ ; the converse is true if and only if  $0 \notin \mathbb{M}$ :

► **Proposition 6.** *Given a monoid  $\mathbb{M}$  of complex linear maps, we have  $\forall D, D', \llbracket D \rrbracket = \llbracket D' \rrbracket \Leftrightarrow V_D = V_{D'}$ , if and only if  $0 \notin \mathbb{M}$ .*

**Proof.** The proof is given in Appendix A.2 ◀

In particular, two diagrams in  $\mathbf{Diag}^{\mathcal{H}}$  have the same action semantics if and only if they have the same quantum semantics.

### 3.2 Interpretation

Given a monoid homomorphism  $\gamma : \mathbf{M} \rightarrow \mathbf{M}'$ , one can transform any  $\mathbf{M}$ -diagram into an  $\mathbf{M}'$ -diagram straightforwardly, by applying  $\gamma$  on each gate of the diagram:

► **Definition 7.** *Given an  $\mathbf{M}$ -diagram  $D : a \rightarrow b$  and a monoid homomorphism  $\gamma : \mathbf{M} \rightarrow \mathbf{M}'$ , we define its  $\gamma$ -interpretation  $\gamma(D) : a \rightarrow b$  as the  $\mathbf{M}'$ -diagram obtained by applying  $\gamma$  to each gate of  $D$ . It is defined inductively as:  $\gamma(\overset{a}{\square}U : a \rightarrow a) = \overset{a}{\square}\gamma(U) : a \rightarrow a$ ; for any other generator  $g$ ,  $\gamma(g) = g$ ;  $\gamma(D_2 \circ D_1) = \gamma(D_2) \circ \gamma(D_1)$ ;  $\gamma(D_1 \oplus D_2) = \gamma(D_1) \oplus \gamma(D_2)$ ; and  $\gamma(\text{Tr}_e(D)) = \text{Tr}_e(\gamma(D))$ .*

► **Proposition 8.** *Any  $\mathbf{M}$ -diagram is the interpretation of an abstract diagram.*

**Proof.** Given an  $\mathbf{M}$ -diagram  $D$ , let  $\mathcal{G}$  be the underlying set of  $\mathbf{M}$  and  $\gamma : \mathcal{G} \rightarrow \mathbf{M}$  s.t.  $\forall U \in \mathcal{G}$ ,  $\gamma(U) = U$ . The function  $\gamma$  can be extended trivially into a homomorphism  $\gamma : \mathcal{G}^* \rightarrow \mathbf{M}$ . Notice that  $D$  can be seen as a (abstract) diagram of  $\mathbf{Diag}^{\mathcal{G}^*}$  and  $\gamma(D) = D$ . ◀

It is easy to see that the action of monoid homomorphisms on diagrams is well-behaved with respect to the semantics:

► **Proposition 9.** *Given any  $\mathbf{M}$ -diagram  $D : a \rightarrow b$  and any monoid homomorphism  $\gamma : \mathbf{M} \rightarrow \mathbf{M}'$ , for any configuration  $(c, p) \in [a]$ , if  $\llbracket D \rrbracket (c, p) = ((c', p'), U)$  then  $\llbracket \gamma(D) \rrbracket (c, p) = ((c', p'), \gamma(U))$ .*

**Proof.** Straightforward by induction. ◀

As a consequence, given two abstract diagrams  $D_1, D_2 \in \mathbf{Diag}^{\mathcal{G}^*}$ , if  $\llbracket D_1 \rrbracket = \llbracket D_2 \rrbracket$  then for any homomorphism  $\gamma : \mathcal{G}^* \rightarrow \mathbf{M}$ ,  $\llbracket \gamma(D_1) \rrbracket = \llbracket \gamma(D_2) \rrbracket$ . The converse is not true in general. Notice that in the framework of graphical languages, an equation holds in graphical languages for traced symmetric (resp. dagger compact closed) monoidal categories if and only if it holds in finite-dimensional vector (resp. Hilbert) spaces [25, 33]. We prove a similar result by showing that interpreting abstract diagrams using 2-dimensional Hilbert spaces is enough to completely characterise their semantics:

► **Proposition 10.** *Given a Hilbert space  $\mathcal{H}$  of dimension at least 2 and a set  $\mathcal{G}$ ,  $\forall D_1, D_2 \in \mathbf{Diag}^{\mathcal{G}^*}$ , there exists a monoid homomorphism  $\gamma : \mathcal{G}^* \rightarrow \mathcal{U}(\mathcal{H})$  s.t.  $\llbracket D_1 \rrbracket = \llbracket D_2 \rrbracket \Leftrightarrow \llbracket \gamma(D_1) \rrbracket = \llbracket \gamma(D_2) \rrbracket$ .*

A stronger version of Proposition 10, where the homomorphism  $\gamma$  is independent of the diagrams, is also true, assuming the axiom of choice:

► **Proposition 11.** *Given a Hilbert space  $\mathcal{H}$  of dimension at least 2, and a set  $\mathcal{G}$  of cardinality at most the cardinality of  $\mathcal{U}(\mathcal{H})$ , there exists a monoid homomorphism  $\gamma : \mathcal{G}^* \rightarrow \mathcal{U}(\mathcal{H})$  s.t.  $\forall D_1, D_2 \in \mathbf{Diag}^{\mathcal{G}^*}$ ,  $\llbracket D_1 \rrbracket = \llbracket D_2 \rrbracket \Leftrightarrow \llbracket \gamma(D_1) \rrbracket = \llbracket \gamma(D_2) \rrbracket$ .*

**Proof of Propositions 10 and 11.** The proof is given in Appendix A.3. ◀

► **Remark 12.** Notice that the cardinality of  $\mathcal{U}(\mathcal{H})$  is  $\max(2^{\aleph_0}, 2^{\dim(\mathcal{H})})$  (where  $2^{\aleph_0}$  is the cardinality of  $\mathbb{R}$  and  $\dim(\mathcal{H})$  is the Hilbert dimension of  $\mathcal{H}$ ).

## 4 Equational Theory

In this section, we introduce an equational theory which allows one to transform any M-diagram into an equivalent one. Indeed, all the equations we present in this section preserve the semantics of the diagrams (see Proposition 14).

These equations are given in Figure 4. They form what we call the CPBS-calculus:

► **Definition 13** (CPBS-calculus). *Two M-diagrams  $D_1, D_2$  are equivalent according to the rules of the CPBS-calculus, denoted  $\text{CPBS} \vdash D_1 = D_2$ , if one can transform  $D_1$  into  $D_2$  using the equations given in Figure 4. More precisely,  $\text{CPBS} \vdash \cdot = \cdot$  is defined as the smallest congruence which satisfies equations of Figure 4 in addition to the axioms of coloured traced prop.*

■ **Figure 4** Axioms of the CPBS-calculus.  $U, V \in M$ . Equations (1) and (2) reflect the monoid structure of  $M$ ; Equations (3) to (5) show how the three generators commute; Equation (6) means that a disconnected diagram (with no inputs/outputs) can be removed; Equations (7) to (10) witness the fact that the negation and the 3-leg PBS are invertible; Equations (11) and (12) are essentially topological rules; Equations (13) to (17) show how 4-leg PBS can be decomposed into 3-leg PBS. Notice in particular that the other rules do not use 4-leg PBS, as a consequence one could define the language using 3-leg PBS only and see the 4-leg PBS as syntactic sugar.

Notice that the CPBS-calculus subsumes the PBS-calculus: the fragment of monochromatic (black)  $\mathbb{C}^{q \times q}$ -diagrams of the CPBS-calculus coincides with the set of PBS-diagrams, moreover, the completeness of both languages implies that for any two PBS-diagrams  $D_1$  and  $D_2$ ,  $\text{PBS} \vdash D_1 = D_2$  if and only if  $\text{CPBS} \vdash D_1 = D_2$ .

► **Proposition 14** (Soundness). *For any two M-diagrams  $D_1$  and  $D_2$ , if  $\text{CPBS} \vdash D_1 = D_2$  then  $\llbracket D_1 \rrbracket = \llbracket D_2 \rrbracket$ .*

**Proof.** Since the semantic equality is a congruence, it suffices to check that for every equation of Figure 4, both sides have the same semantics, which is easy to do. ◀

We introduce normal forms, that will be useful to prove that the equational theory is complete, and will also play a role in optimising the number of gates in a diagram in Section 5.





■ **Figure 5** An example of a diagram (left) and its equivalent diagram in normal form (right).

► **Definition 15.** A diagram is said to be in normal form if it is of the form  $M \circ P \circ F \circ G \circ S$ , where:

- $S$  is of the form  $b_1 \oplus \dots \oplus b_n$ , where each  $b_i$  is either  $\underline{v}$ ,  $\underline{h}$  or  $\overline{\diamond}$
- $G$  is of the form  $g_1 \oplus \dots \oplus g_k$ , where each  $g_i$  is either  $\underline{v}$ ,  $\underline{h}$ ,  $\underline{v} \boxed{U_i}$  or  $\underline{h} \boxed{U_i}$ , with  $U_i \neq I$
- $F$  is of the form  $n_1 \oplus \dots \oplus n_k$ , where each  $n_i$  is either  $\underline{v}$ ,  $\underline{h}$ ,  $\underline{v} \ominus$  or  $\underline{h} \ominus$
- $P$  is a permutation of the wires, that is, a trace-free diagram in which all generators are identity wires or swaps
- $M$  is of the form  $w_1 \oplus \dots \oplus w_m$ , where each  $w_i$  is either  $\underline{v}$ ,  $\underline{h}$  or  $\overline{\diamond}$ .

For example, the diagram shown in Figure 3 (right) is in normal form.

► **Theorem 16.** For any M-diagram  $D$ , there exists an M-diagram in normal form  $N$  such that  $\text{CPBS} \vdash D = N$ .

**Proof.** The proof is given in Appendix A.4. ◀

Note that the structure of the normal form as well as the proof of Theorem 16 use in an essential way the removal of useless wires made possible by the use of colours, and in particular Equation (10), which has no equivalent in the monochromatic PBS-calculus of [13]. An example of a diagram and its normal form are given in Figure 5.

Now we use the normal form to prove the completeness of the CPBS-calculus:

► **Lemma 17** (Uniqueness of the normal form). For any two diagrams in normal form  $N$  and  $N'$ , if  $\llbracket N \rrbracket = \llbracket N' \rrbracket$  then  $N = N'$ .

**Proof.** The proof is given in Appendix A.5. ◀

► **Theorem 18** (Completeness). Given any two M-diagrams  $D_1$  and  $D_2$ , if  $\llbracket D_1 \rrbracket = \llbracket D_2 \rrbracket$  then  $\text{CPBS} \vdash D_1 = D_2$ .

**Proof.** By Theorem 16, there exist  $N_1, N_2$  in normal form such that  $\text{CPBS} \vdash D_1 = N_1$  and  $\text{CPBS} \vdash D_2 = N_2$ . By Proposition 14,  $\llbracket N_1 \rrbracket = \llbracket D_1 \rrbracket = \llbracket D_2 \rrbracket = \llbracket N_2 \rrbracket$ . Therefore, by Lemma 17,  $N_1 = N_2$ . By transitivity, this proves that  $\text{CPBS} \vdash D_1 = D_2$ . ◀

Finally, each equation of Figure 4 is necessary for the completeness:

► **Theorem 19** (Minimality). None of the equations of Figure 4 is a consequence of the others.

**Proof.** The proof is given in Appendix A.6. ◀

## 5 Resource Optimisation

We show in this section that the equational theory of the CPBS-calculus can be used for resource optimisation.

## 5.1 Minimising the Number of Oracle Queries

We consider the problem of minimising the number of oracle queries: given a set  $\mathcal{G}$  of (distinct) oracles and a  $\mathcal{G}^*$ -diagram  $D$ , the objective is to find a diagram  $D'$  equivalent to  $D$  (i.e.  $\llbracket D \rrbracket = \llbracket D' \rrbracket$ ) such that  $D'$  uses a minimal number of queries to each oracle. Since there are several oracles, the definition of the optimal diagrams should be made precise.

First, we define the number of queries to a given oracle:

► **Definition 20.** *Given a  $\mathcal{G}^*$ -diagram  $D$ , for any  $U \in \mathcal{G}$ , let  $\#_U(D)$  be the number of queries to  $U$  in  $D$ , inductively defined as follows:  $\#_U(\overset{a}{\square}w\text{---}) = |w|_U$ ;  $\#_U(g) = 0$  for all the other generators;  $\#_U(D_1 \oplus D_2) = \#_U(D_2 \circ D_1) = \#_U(D_1) + \#_U(D_2)$ ; and  $\#_U(\text{Tr}_a(D)) = \#_U(D)$ , where  $|w|_U$  is the number of occurrences of  $U$  in the word  $w \in \mathcal{G}^*$ .*

We can now define a query-optimal diagram as follows:

► **Definition 21.** *A  $\mathcal{G}^*$ -diagram  $D$  is query-optimal if  $\forall D' \in \text{Diag}^{\mathcal{G}^*}, \forall U \in \mathcal{G}, \llbracket D \rrbracket = \llbracket D' \rrbracket$  implies  $\#_U(D) \leq \#_U(D')$ .*

Note that given a diagram, it is not *a priori* guaranteed that there exists an equivalent diagram which is query-optimal: for instance, it might be that all the diagrams which minimise the number of queries to some oracle  $U$  do not minimise the number of queries to another oracle  $V$ . We actually show (Proposition 23) that any diagram can be turned into a query-optimal one. To this end, we first need a lower bound on the number of queries to a given oracle:

► **Proposition 22 (Lower bound).** *For any  $\mathcal{G}^*$ -diagram  $D : a \rightarrow b$  and any  $U \in \mathcal{G}$ ,  $\#_U(D) \geq \left\lceil \sum_{(c,p) \in [a]} \frac{|w_{c,p}^D|_U}{2} \right\rceil$  where  $w_{c,p}^D \in \mathcal{G}^*$  is such that  $\llbracket D \rrbracket(c,p) = ((c',p'), w_{c,p}^D)$ .*

**Proof.** Notice that each gate  $\overset{a}{\square}w\text{---}$  of the diagram  $D$  is used at most twice according to the semantics,<sup>3</sup> in other words, there are either at most two pairs  $(c,p), (c',p')$  such that  $w$  contributes once to  $w_{c,p}^D$  and once to  $w_{c',p'}^D$ ; or at most a single pair  $(c,p)$  such that  $w$  contributes twice to  $w_{c,p}^D$ . As a consequence,  $\sum_{(c,p) \in [a]} |w_{c,p}^D|_U \leq 2\#_U(D)$ , which leads to the lower bound. ◀

Note that Proposition 22 provides a lower bound on the minimal number of queries to  $U$  one can reach in optimising a diagram since the right-hand side of the inequality only depends on the semantics of the diagram.

We are now ready to introduce an optimisation procedure that transforms any diagram into an equivalent query-optimal one:

### Query optimisation procedure of a $\mathcal{G}^*$ -diagram $D$ :

1. Transform  $D$  into its normal form  $D_{NF}$ . A recursive procedure for doing this can easily be deduced from the proof of Theorem 16 (given in Appendix A.4).
2. Split all gates into elementary gates (that is, gates whose label is a single letter), using the following variants of Equation (2), which are consequences of the equations of Figure 4 (see Appendix B):  $\forall U \in \mathcal{G}, \forall w \in \mathcal{G}^*, w \neq I$ :

<sup>3</sup> This can be stated more formally by replacing the contents of the gates by distinct names in order to get a (coloured) bare diagram (see [8]), and then proved in a similar way as Proposition 3 of [8].

$$\begin{array}{c} \text{v} \\ \hline \boxed{wU} \end{array} \rightarrow \begin{array}{c} \text{v} \\ \hline \boxed{U} \end{array} \begin{array}{c} \text{w} \\ \hline \boxed{w} \end{array} \quad (18) \quad \begin{array}{c} \text{h} \\ \hline \boxed{wU} \end{array} \rightarrow \begin{array}{c} \text{h} \\ \hline \boxed{U} \end{array} \begin{array}{c} \text{w} \\ \hline \boxed{w} \end{array} \quad (19) \quad \begin{array}{c} \text{---} \\ \hline \boxed{wU} \end{array} \rightarrow \begin{array}{c} \text{---} \\ \hline \boxed{U} \end{array} \begin{array}{c} \text{---} \\ \hline \boxed{w} \end{array} \quad (20)$$

3. As long as the diagram contains two non-black gates with the same label, merge them. To do so, deform the diagram to put one over the other, and apply one of the following equations, which are also consequences of the equations of Figure 4:

$$\begin{array}{c} \text{v} \\ \hline \boxed{U} \\ \text{h} \\ \hline \boxed{U} \end{array} \rightarrow \begin{array}{c} \text{v} \\ \hline \text{---} \\ \text{h} \\ \hline \text{---} \end{array} \begin{array}{c} \text{---} \\ \hline \text{---} \end{array} \begin{array}{c} \text{---} \\ \hline \boxed{U} \\ \text{---} \\ \hline \text{---} \end{array} \quad (21) \quad \begin{array}{c} \text{h} \\ \hline \boxed{U} \\ \text{v} \\ \hline \boxed{U} \end{array} \rightarrow \begin{array}{c} \text{h} \\ \hline \text{---} \\ \text{v} \\ \hline \text{---} \end{array} \begin{array}{c} \text{---} \\ \hline \text{---} \end{array} \begin{array}{c} \text{---} \\ \hline \boxed{U} \\ \text{---} \\ \hline \text{---} \end{array} \quad (22)$$

$$\begin{array}{c} \text{v} \\ \hline \boxed{U} \\ \text{v} \\ \hline \boxed{U} \end{array} \rightarrow \begin{array}{c} \text{v} \\ \hline \text{---} \\ \text{v} \\ \hline \text{---} \end{array} \begin{array}{c} \text{---} \\ \hline \text{---} \end{array} \begin{array}{c} \text{---} \\ \hline \boxed{U} \\ \text{---} \\ \hline \text{---} \end{array} \quad (23) \quad \begin{array}{c} \text{h} \\ \hline \boxed{U} \\ \text{h} \\ \hline \boxed{U} \end{array} \rightarrow \begin{array}{c} \text{h} \\ \hline \text{---} \\ \text{h} \\ \hline \text{---} \end{array} \begin{array}{c} \text{---} \\ \hline \text{---} \end{array} \begin{array}{c} \text{---} \\ \hline \boxed{U} \\ \text{---} \\ \hline \text{---} \end{array} \quad (24)$$

An example of query-optimised diagram is given in Figure 9. The query-optimisation procedure transforms any diagram into an equivalent query-optimal one:

► **Proposition 23.** *The diagram  $D_0$  output by the query optimisation procedure is query-optimal: for any  $U$  and any  $D'$  s.t.  $\llbracket D' \rrbracket = \llbracket D_0 \rrbracket$ , one has  $\#_U(D_0) \leq \#_U(D')$ .*

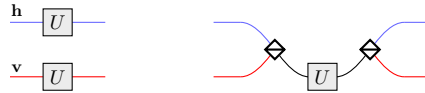
**Proof.** Notice that in  $D_{NF}$ , for each gate there is one and only one input state  $(c, p)$  which goes to this gate. As a consequence,  $\forall U, \#_U(D_{NF}) = \sum_{(c,p) \in [a]} |w_{c,p}^D|_U$  (where  $D_{NF} : a \rightarrow b$ ). Moreover,  $\forall U, \#_U(D_0) = \left\lceil \frac{\#_U(D_{NF})}{2} \right\rceil$ , thus  $D_0$  meets the lower bound of Proposition 22 and hence is query-optimal. ◀

Note that the query-optimisation procedure is efficient: one can naturally define the size  $|D|$  of a diagram  $D \in \text{Diag}^{G^*}$  as follows:  $|a \boxed{w}| = |w|$ ;  $|g| = 1$  for all the other generators;  $|D_1 \oplus D_2| = |D_2 \circ D_1| = |D_1| + |D_2|$ ; and  $|Tr_a(D)| = |D| + 1$ . Step 1 of the procedure, which consists in putting the diagram in normal form, can be done using a number of elementary equations of Figure 4 which is quadratic in the size of the diagram, the other two steps being linear. Notice that here we only count the number of basic equations. The procedure also requires some diagrammatic transformations (that is, deformations), which can be handled efficiently (more precisely, at most in quadratic time) using appropriate data structures.

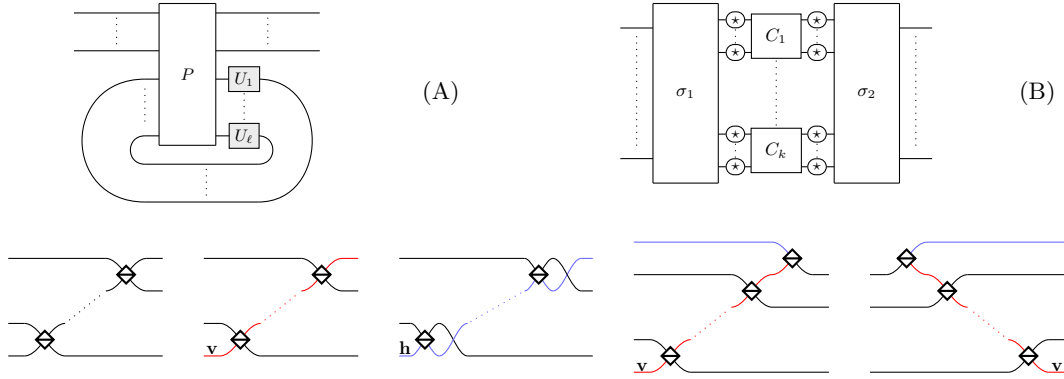
## 5.2 Optimising Both Queries and PBS

We refine the resource optimisation of a diagram by considering not only the number of queries but also the number of instructions, and in particular the number of polarising beam splitters. Note that the number of beam splitters and the number of queries cannot be minimised independently, in the sense that there might not exist a diagram that is both query-optimal and PBS-optimal (see such an example in Figure 6). As the implementation of an oracle is *a priori* more expensive than the implementation of a single PBS, we optimise the number of queries and then the number of PBS in this order, i.e. the measure of complexity is the lexicographic order number of queries, number of polarising beam splitters.

► **Definition 24.** *A diagram  $D$  is query-PBS-optimal if  $D$  is query-optimal and for any query-optimal diagram  $D'$  equivalent to  $D$  (i.e.  $\llbracket D \rrbracket = \llbracket D' \rrbracket$ ),  $\#_{\text{PBS}}(D) \leq \#_{\text{PBS}}(D')$ , where  $\#_{\text{PBS}}(D)$  be the number of PBS of  $D$ .*



■ **Figure 6** Two equivalent diagrams: the diagram on the left is optimal in terms of the number of polarising beam splitters, the diagram on the right is optimal in terms of queries. Note that there is no equivalent diagram with no polarising beam splitter and at most a single query.



■ **Figure 7** Schematic description of a diagram in PGT form (for Permutation, Gates and Traces). A diagram is in PGT form if it is of the form (A), with  $P$  of the form (B), and the  $C_i$  of the forms depicted on the second line.  $\text{--}(\star)\text{--}$  denotes either  $\overset{a}{\text{--}}\text{--}$  or  $\overset{a}{\text{--}}\text{--}(\ominus)\text{--}$  with  $a \in \{\mathbf{v}, \mathbf{h}\}$ , and  $\sigma_1, \sigma_2$  are permutations of the wires.

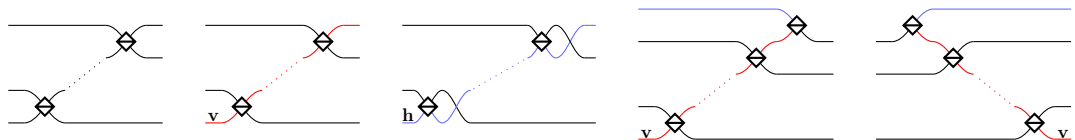
We introduce an efficient heuristic, called *PGT procedure* that, when applied on a query-optimal diagram  $D_0$ , preserves the number of queries. The produced diagram, called in PGT form (see Figure 7), contains at most as many PBS as the original diagram, and moreover is query-PBS-optimal when there is at most one query to each oracle (see Proposition 30 and Theorem 31).

More precisely, the PGT procedure consists in putting  $D_0$  in the so-called PGT form, which we prove to contain few PBS. First, we consider query-free diagrams:

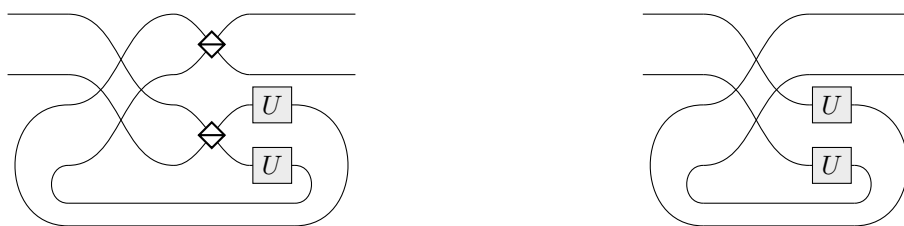
► **Definition 25.** *A diagram  $D$  is in stair form if it is of the form*



where  $\sigma_1$  and  $\sigma_2$  are permutations of the wires,  $\text{--}(\star)\text{--}$  denotes either  $\overset{a}{\text{--}}\text{--}$  or  $\overset{a}{\text{--}}\text{--}(\ominus)\text{--}$  with  $a \in \{\mathbf{v}, \mathbf{h}\}$ , and  $C_1, \dots, C_k$  are each of one of the following forms:



The diagrams of these forms will be called staircases. The  $C_i$  will be called the staircases of  $D$ .



■ **Figure 8** [Left] An example of diagram in PGT form which is optimal in the number of queries but not in the number of polarising beam splitters. Indeed it is equivalent to the diagram on the right which is query-optimal and PBS-free.

► **Remark 26.** Note that in the diagram (B), all wires can be of arbitrary colours. We did not represent the labels in order to not overload the figures.

Diagrams in stair form are optimal in terms of the number of polarising beam splitters:

► **Theorem 27.** Any diagram  $D : a \rightarrow b$  in stair form is PBS-optimal (that is, for any diagram  $D' : a \rightarrow b$ ,  $\llbracket D \rrbracket = \llbracket D' \rrbracket \Rightarrow \#_{\text{PBS}}(D) \leq \#_{\text{PBS}}(D')$ ).

**Proof.** The proof is given in Appendix A.7. ◀

We extend the stair form to diagrams with queries as follows, leading to the PGT form (for Permutation/Gates/Traces):

► **Definition 28.** A  $\mathcal{G}^*$ -diagram is in PGT form (for Permutation, Gates and Traces) if it is of the form

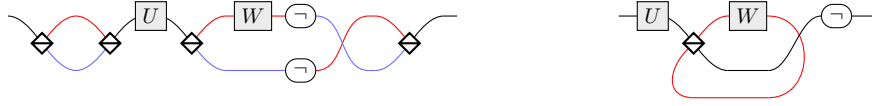


where  $P$  is in stair form and  $U_1, \dots, U_\ell \in \mathcal{G}$ .

► **Remark 29.** Like in the diagram (B), all wires of (A) can be of arbitrary colours.

Contrary to the stair form, the PGT form is not optimal (see as an example Figure 8). Intuitively, if there are several queries to an oracle  $U$ , then decomposing the corresponding gates into blue and red gates and then recomposing them in a different way may lead to a diagram with a smaller number of PBS. However, we will prove that applying the PGT procedure after the query optimisation procedure gives us a query-PBS-optimal diagram when there is at most one query to each oracle (see Theorem 31).

The procedure relies on equations of Figure 4, together with easy to derive variants of these equations. The derivations of the additional equations are given in Appendix C.2. The procedure, with all steps detailed, more pictures and explicit statement of the variants of the equations, is given in Appendix C.1.

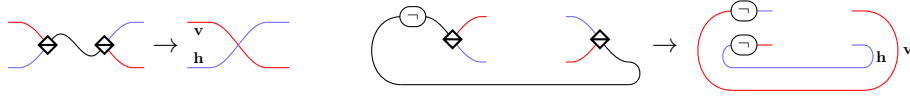


■ **Figure 9** The diagram on the left is the obtained by applying the query-optimisation procedure on the example of Figure 5. The diagram on the right is (up to deformation) obtained by applying the PGT procedure to the diagram on the left. Note that this diagram is both query- and PBS-optimal.

### PGT procedure:

Given a query-optimal diagram  $D_0$ :

0. During all the procedure, every time there are two consecutive negations, we remove them using Equation (7), (8) or their all-black version.
1. Deform the query-optimal diagram  $D_0$  to put it in the form (A) with  $P$  gate-free. The goal of the following steps is to put  $P$  in stair form.
2. Split all PBS of the form  $\begin{matrix} a \\ b \end{matrix} \diamond$  into combinations of  $\begin{matrix} \text{red} \\ \text{blue} \end{matrix} \diamond$ ,  $\begin{matrix} \text{blue} \\ \text{red} \end{matrix} \diamond$ ,  $\begin{matrix} \text{red} \\ \text{red} \end{matrix} \diamond$  and  $\begin{matrix} \text{blue} \\ \text{blue} \end{matrix} \diamond$ , using Equations (13) to (17).
3. As long as there are two PBS connected by a black wire, with possibly a black negation on this wire, push the possibly remaining negation out using Equation (4), and cancel the PBS together using Equation (10) and its variants. For example:



When there are not two such PBS anymore, all black wires are connected to at least one side of  $P$  (possibly through negations), and the PBS are connected together with red and blue wires with possibly negations on them.

4. Remove all isolated loops. Note that since  $D_0$  is query-optimal, there cannot be loops containing gates at this point.

5. Deform  $P$  to put it in the form(B) with the  $C_i$  of the form  $\begin{matrix} \text{red} \\ \text{blue} \end{matrix} \diamond \begin{matrix} \text{red} \\ \text{blue} \end{matrix} \diamond$  and  $\sigma_1$  and

$\sigma_2$  being wire permutations, where  $\begin{matrix} \text{red} \\ \text{blue} \end{matrix} \diamond \begin{matrix} \text{red} \\ \text{blue} \end{matrix} \diamond$  is either  $\begin{matrix} \text{red} \\ \text{red} \end{matrix} \diamond$  or  $\begin{matrix} \text{blue} \\ \text{blue} \end{matrix} \diamond$  and  $\begin{matrix} \text{red} \\ \text{blue} \end{matrix} \diamond$  is either  $\begin{matrix} \text{red} \\ \text{blue} \end{matrix} \diamond$  or  $\begin{matrix} \text{blue} \\ \text{red} \end{matrix} \diamond$ .

6. Remove the negations in the middle of the  $C_i$  by pushing them to the bottom by means of variants of Equation (4).
7. Transform each  $C_i$ , which is now, up to deformation, a ladder of PBS without negations, into one of the five kinds of stairs depicted in Definition 25, depending on its type. To do so, deform it and apply Equations (11) and (12) appropriately, and repeatedly apply the appropriate equation among (14), (15), (16), and a variant of (13). This gives us  $D_1$ .

An example of diagram produced by the PGT procedure is given in Figure 9.

Since the PGT procedure consists in putting a subdiagram of  $D_0$  in stair form (except Step 1 which is just deformation and does not change the number of PBS), Theorem 27 implies in particular that this procedure does not increase the number of PBS in  $D_0$ :

► **Proposition 30.** *The diagram  $D_1$  output by the PGT procedure contains at most as many PBS as the initial diagram  $D_0$ .*

This also implies that given any diagram  $D$ , there exists an equivalent query-PBS-optimal diagram in PGT form. Indeed, by Proposition 23, there exist query-optimal diagrams equivalent to  $D$ , and among these diagrams, some of them have minimal number of PBS and are therefore query-PBS-optimal. Finally, applying the PGT procedure to one of these diagrams gives us an equivalent diagram in PGT form, which, since the PGT procedure does not change the gates or increase the number of PBS, is still query-PBS-optimal.

Applying the PGT procedure after the query optimisation procedure produces an interesting heuristic: the output diagram is necessarily query-optimal and, although it is not necessarily query-PBS-optimal in general, it is whenever it does not contain two queries to the same oracle:

► **Theorem 31.** *Given a diagram  $D_1$  obtained by applying first the query optimisation procedure then the PGT procedure to a diagram  $D$ , if  $D_1$  does not contain two queries to the same oracle (i.e.  $\forall U \in \mathcal{G}, \#_U(D_1) \leq 1$ ), then it is query-PBS-optimal.*

**Proof.** The proof is given in Appendix A.8. ◀

Finally, note that, like the query optimisation procedure, the PGT procedure is efficient: it can be done using a number of elementary graphical transformations (those of Figure 4) which is linear in the size of the diagram. It also requires some diagrammatic transformations, which can be handled using appropriate data structures, leading to a quadratic algorithm.

### 5.3 Hardness

We show in this section that the query-PBS optimisation problem is actually NP-hard.

► **Theorem 32.** *The problem of, given an abstract diagram, finding an equivalent query-PBS-optimal diagram, is NP-hard.*

The proof, given in Appendix A.9.1, is based on a reduction from the maximum Eulerian cycle decomposition problem (MAX-ECD) which is known to be NP-hard [9]. The MAX-ECD problem consists, given a graph, in finding a partition of its set of edges into the maximum number of cycles. Intuitively, the reduction goes as follows: given an Eulerian graph  $G = (V = \{v_0, \dots, v_{n-1}\}, E)$ , let  $\sigma$  be a permutation of the vertices of the graph s.t.  $\forall i, (v_i, \sigma(v_i)) \in E$  (such a  $\sigma$  exists since  $G$  is Eulerian), we construct a  $V^*$ -diagram  $D$  such that the number of occurrences of each  $v_i$  in  $D$  is half its degree in  $G$ ; and such that  $\forall i, \llbracket D \rrbracket(\mathbf{V}, i) = ((\mathbf{V}, i), v_i)$  and  $\llbracket D \rrbracket(\mathbf{H}, i) = ((\mathbf{H}, i), \sigma(v_i))$ . Roughly speaking, we show that the edge-partitions of  $G$  into cycles correspond to the possible implementations of  $D$ , and that an implementation with a minimal number of PBS leads to a partition with a maximal number of cycles.

In the following, we explore a few variants of the problem, which remain NP-hard.

First, query-PBS optimisation is still hard when restricted to negation-free diagrams:

► **Corollary 33.** *The problem of, given a negation-free abstract diagram, finding an equivalent diagram which is query-PBS-optimal among negation-free diagrams, is NP-hard.*

**Proof.** The proof is given in Appendix A.9.2. ◀

Additionally, it is also hard, in a query-optimal diagram, to optimise the PBS and the negations together, respectively: with respect to a cost function (at least in the case where the cost of a negation is not less than the cost of a PBS); with the negations prioritised over the PBS; and with the PBS prioritised over the negations. Note that the NP-hardness is clear

in the third case since the considered problem is a refinement of the query-PBS-optimisation problem addressed in Theorem 32.

► **Corollary 34.** *For any  $\alpha \geq 1$ , the problem of, given an abstract diagram  $D$ , finding an equivalent query-optimal diagram  $D'$  such that  $\#_{\text{PBS}}(D') + \alpha\#_{\neg}(D')$  is minimal, is NP-hard, where  $\#_{\neg}(D)$  is the number of negations in  $D$ .*

**Proof.** The proof is given in Appendix A.9.3. ◀

Although we were only able to prove Corollary 34 for  $\alpha \geq 1$ , we conjecture that the optimisation is actually NP-hard even if the negations cost less than the PBS:

► **Conjecture 35.** *For any  $\alpha \geq 0$ , the problem of, given an abstract diagram  $D$ , finding an equivalent query-optimal diagram  $D'$  such that  $\#_{\text{PBS}}(D') + \alpha\#_{\neg}(D')$  is minimal, is NP-hard.*

► **Corollary 36.** *The problem of, given an abstract diagram  $D$ , finding an equivalent query- $\neg$ -PBS-optimal<sup>4</sup> diagram is NP-hard.*

**Proof.** The NP-hardness of this problem directly follows from Corollary 33. Indeed, given a negation-free diagram  $D$ , the query optimisation procedure gives us a negation-free query-optimal diagram  $D'$  equivalent to  $D$ . Any query- $\neg$ -PBS-optimal diagram equivalent to  $D$  has to contain at most as many negations as  $D'$ , namely 0, that is, be negation-free. Thus, finding a query- $\neg$ -PBS-optimal equivalent to  $D$  amounts to finding a negation-free query-PBS-optimal diagram equivalent to  $D$ . ◀

Finally, as noted above, the NP-hardness when the PBS are prioritised over the negations is a direct consequence of Theorem 32:

► **Remark 37.** The problem of, given an abstract diagram  $D$ , finding an equivalent query-PBS- $\neg$ -optimal diagram is NP-hard.

## 6 Discussions and Future Work

The power and limits of quantum coherent control is an intriguing question. Maybe surprisingly,<sup>5</sup> we have proved that coherently controlled quantum computations, when expressed in the PBS-calculus, can be efficiently optimised: any PBS-diagram can be transformed in polynomial time into a diagram that is optimal in terms of oracle queries. We have refined the procedure to also decrease the number of polarising beam splitters. It leads to an optimal diagram when each oracle is queried only once, but the corresponding optimisation problem is NP-hard in general. We leave to future work an experimental evaluation of the PGT procedure when each oracle is not necessarily queried only once.

It might be that the NP-hardness result is even more significant than the optimisation heuristic, as the hardness might scale up as the language is further developed. There is however no certainty that things will necessarily happen as badly, and it might be a perspective for further developments of this language to find extensions of it in which such optimisation problems are easy to solve.

<sup>4</sup> A diagram is query- $\neg$ -PBS-optimal if it is optimal according to the lexicographic order: the number of queries then the number of negations and finally the number of polarising beam splitters. The definition of a query-PBS- $\neg$ -optimal diagram is analogous.

<sup>5</sup> One may argue that this could be due to the simplicity of the language. It belongs to future work to know whether things would be as simple if the language were to be extended to allow for a more general quantum control.



To perform the resource optimisation, we have introduced a few add-ons to the framework of the PBS-calculus. First, we have refined the syntax in order to allow the representation of unsaturated (or 3-leg) polarising beam splitters. They are essential ingredients for resource optimisation, as they provide a way to decompose a diagram into elementary components and then remove the useless ones. However, note that one can perform resource optimisation of vanilla PBS-diagrams, using the refined one only as an intermediate language. Indeed, given a vanilla PBS-diagram (where all wires are black), one can apply the optimisation procedures described in this paper. The resulting optimised PBS-diagram may contain some unsaturated PBS, but all these 3-leg PBS can be saturated by adding useless traces and then one can make the diagram monochromatic. The resulting vanilla PBS-diagram keeps the same number of queries and PBS.

We have also generalised the gates of the diagrams, by considering arbitrary monoids. This is a natural abstraction that allows one to consider various examples and in particular the one of the free monoid which is appropriate to model the oracle queries. The query complexity is a convenient model to prove lower bounds, but note that the optimisation procedures described in this paper can be applied with any arbitrary monoid (for instance using Proposition 8). However, there is no guarantee of minimality with an arbitrary monoid.

Another direction of research is to consider resource optimisation in a more expressive language for quantum control. Indeed, the polarisation of a particle can only be flipped within a PBS-diagram. The PBS-calculus is well suited for most applications of coherent control in quantum computing, by allowing the description of superpositions of classical controls (in particular superposition of causal orders) since the input particle can be in any superposition of polarisations. However, it would be interesting to develop resource optimisation techniques for quantum computation involving arbitrary quantum control.

---

## References

- 1 Alastair A. Abbott, Julian Wechs, Dominic Horsman, Mehdi Mhalla, and Cyril Branciard. Communication through coherent control of quantum channels. *Quantum*, 4:333, September 2020. [arXiv:1810.09826](#), [doi:10.22331/q-2020-09-24-333](#).
- 2 Thorsten Altenkirch and Jonathan Grattage. A functional quantum programming language. In *20th Annual IEEE Symposium on Logic in Computer Science (LICS'05)*, pages 249–258. IEEE, 2005.
- 3 Amihoud Amir, Tzvikia Hartman, Oren Kapah, Avivit Levy, and Ely Porat. On the cost of interchange rearrangement in strings. *SIAM Journal on Computing*, 39(4):1444–1461, 2010. [doi:10.1137/080712969](#).
- 4 Matthew Amy, Dmitri Maslov, and Michele Mosca. Polynomial-time T-depth optimization of Clifford+T circuits via matroid partitioning. *IEEE Transactions on Computer-Aided Design of Integrated Circuits and Systems*, 33(10):1476–1489, 2014.
- 5 Mateus Araújo, Fabio Costa, and Časlav Brukner. Computational advantage from quantum-controlled ordering of gates. *Physical Review Letters*, 113(25):250402, 2014. [arXiv:1401.8127](#), [doi:10.1103/PhysRevLett.113.250402](#).
- 6 Pablo Arrighi, Christopher Cedzich, Marin Costes, Ulysse Rémond, and Benoît Valiron. Addressable quantum gates. *ACM Transactions on Quantum Computing*, 4(3), April 2023. [doi:10.1145/3581760](#).
- 7 Costin Badescu and Prakash Panangaden. Quantum alternation: Prospects and problems. In Chris Heunen, Peter Selinger, and Jamie Vicary, editors, *Proceedings 12th International Workshop on Quantum Physics and Logic, QPL 2015, Oxford, UK, July 15-17, 2015*, volume 195 of *EPTCS*, pages 33–42, 2015. [doi:10.4204/EPTCS.195.3](#).
- 8 Cyril Branciard, Alexandre Clément, Mehdi Mhalla, and Simon Perdrix. Coherent control and distinguishability of quantum channels via PBS-diagrams. In Filippo Bonchi and Simon J.

- Puglisi, editors, *46th International Symposium on Mathematical Foundations of Computer Science (MFCS 2021)*, volume 202 of *Leibniz International Proceedings in Informatics (LIPIcs)*, pages 22:1–22:20, Dagstuhl, Germany, August 2021. Schloss Dagstuhl – Leibniz-Zentrum für Informatik. URL: <https://hal.science/hal-03325456>, arXiv:2103.02073, doi:10.4230/LIPIcs.MFCS.2021.22.
- 9 Alberto Caprara. Sorting permutations by reversals and Eulerian cycle decompositions. *SIAM Journal on Discrete Mathematics*, 12(1):91–110, 1999. doi:10.1137/S089548019731994X.
  - 10 Giulio Chiribella. Perfect discrimination of no-signalling channels via quantum superposition of causal structures. *Physical Review A*, 86(4):040301, 2012. arXiv:1109.5154, doi:10.1103/PhysRevA.86.040301.
  - 11 Giulio Chiribella, Giacomo Mauro D’Ariano, Paolo Perinotti, and Benoît Valiron. Quantum computations without definite causal structure. *Physical Review A*, 88:022318, August 2013. arXiv:0912.0195, doi:10.1103/PhysRevA.88.022318.
  - 12 Alexandre Clément, Nicolas Heurtel, Shane Mansfield, Simon Perdrix, and Benoît Valiron. LO<sub>v</sub>-calculus: A graphical language for linear optical quantum circuits. In Stefan Szeider, Robert Ganian, and Alexandra Silva, editors, *47th International Symposium on Mathematical Foundations of Computer Science (MFCS 2022)*, volume 241 of *Leibniz International Proceedings in Informatics (LIPIcs)*, pages 35:1–35:16, Dagstuhl, Germany, 2022. Schloss Dagstuhl – Leibniz-Zentrum für Informatik. URL: <https://hal.science/hal-03926660>, arXiv:2204.11787, doi:10.4230/LIPIcs.MFCS.2022.35.
  - 13 Alexandre Clément and Simon Perdrix. PBS-calculus: A graphical language for coherent control of quantum computations. In Javier Esparza and Daniel Král, editors, *45th International Symposium on Mathematical Foundations of Computer Science (MFCS 2020)*, volume 170 of *Leibniz International Proceedings in Informatics (LIPIcs)*, pages 24:1–24:14, Dagstuhl, Germany, August 2020. Schloss Dagstuhl–Leibniz-Zentrum für Informatik. URL: <https://hal.science/hal-02929291>, arXiv:2002.09387, doi:10.4230/LIPIcs.MFCS.2020.24.
  - 14 Alexandre Clément. *Graphical Languages for Quantum Control and Linear Optics*. PhD thesis, Université de Lorraine, May 2023. URL: <http://www.theses.fr/en/2023LORR0093>.
  - 15 Timoteo Colnaghi, Giacomo Mauro D’Ariano, Stefano Facchini, and Paolo Perinotti. Quantum computation with programmable connections between gates. *Physics Letters A*, 376(45):2940–2943, 2012. arXiv:1109.5987, doi:10.1016/j.physleta.2012.08.028.
  - 16 Alejandro Díaz-Caro, Mauricio Guillermo, Alexandre Miquel, and Benoît Valiron. Realizability in the unitary sphere. In *2019 34th Annual ACM/IEEE Symposium on Logic in Computer Science (LICS)*, pages 1–13. IEEE, 2019.
  - 17 Gilles Dowek and Pablo Arrighi. Lineal: A linear-algebraic lambda-calculus. *Logical Methods in Computer Science*, 13, 2017.
  - 18 Daniel Ebler, Sina Salek, and Giulio Chiribella. Enhanced communication with the assistance of indefinite causal order. *Physical Review Letters*, 120(12):120502, March 2018. arXiv:1711.10165, doi:10.1103/PhysRevLett.120.120502.
  - 19 Stefano Facchini and Simon Perdrix. Quantum circuits for the unitary permutation problem. In *International Conference on Theory and Applications of Models of Computation*, pages 324–331. Springer, 2015. arXiv:1405.5205, doi:10.1007/978-3-319-17142-5\_28.
  - 20 Adrien Feix, Mateus Araújo, and Časlav Brukner. Quantum superposition of the order of parties as a communication resource. *Physical Review A*, 92(5):052326, 2015. arXiv:1508.07840, doi:10.1103/PhysRevA.92.052326.
  - 21 Herbert Fleischner. *Eulerian Graphs and Related Topics*, volume 50 of *Annals of Discrete Mathematics*. Elsevier, 1991. URL: <https://www.elsevier.com/books/eulerian-graphs-and-related-topics/fleischner/978-0-444-89110-5>.
  - 22 Brett Giles and Peter Selinger. Remarks on Matsumoto and Amano’s normal form for single-qubit Clifford+*T* operators, 2019. arXiv:1312.6584.
  - 23 Philippe Allard Guérin, Adrien Feix, Mateus Araújo, and Časlav Brukner. Exponential communication complexity advantage from quantum superposition of the direction

- of communication. *Physical Review Letters*, 117(10):100502, 2016. [arXiv:1605.07372](#), [doi:10.1103/PhysRevLett.117.100502](#).
- 24 Lucien Hardy. Probability theories with dynamic causal structure: a new framework for quantum gravity. *arXiv preprint gr-qc/0509120*, 2005.
  - 25 Masahito Hasegawa, Martin Hofmann, and Gordon Plotkin. Finite dimensional vector spaces are complete for traced symmetric monoidal categories. In *Pillars of computer science*, pages 367–385. Springer, 2008.
  - 26 Ian Holyer. The NP-completeness of some edge-partition problems. *SIAM Journal on Computing*, 10(4):713–717, 1981. [doi:10.1137/0210054](#).
  - 27 Vadym Kliuchnikov and Dmitri Maslov. Optimization of Clifford circuits. *Physical Review A*, 88(5):052307, 2013.
  - 28 Saunders MacLane. Categorical algebra. *Bulletin of the American Mathematical Society*, 71(1):40–106, 1965.
  - 29 Ken Matsumoto and Kazuyuki Amano. Representation of quantum circuits with Clifford and  $\pi/8$  gates, 2008. [arXiv:0806.3834](#).
  - 30 Yunseong Nam, Neil J. Ross, Yuan Su, Andrew M. Childs, and Dmitri Maslov. Automated optimization of large quantum circuits with continuous parameters. *npj Quantum Information*, 4(1):1–12, 2018.
  - 31 Ognjan Oreshkov, Fabio Costa, and Časlav Brukner. Quantum correlations with no causal order. *Nature communications*, 3(1):1–8, 2012.
  - 32 Martin J. Renner and Časlav Brukner. Reassessing the computational advantage of quantum-controlled ordering of gates. *Physical Review Research*, 3(4):043012, 2021.
  - 33 Peter Selinger. Finite dimensional hilbert spaces are complete for dagger compact closed categories. *Electronic Notes in Theoretical Computer Science*, 270(1):113–119, 2011.
  - 34 Augustin Vanrietvelde, Hlér Kristjánsson, and Jonathan Barrett. Routed quantum circuits. *Quantum*, 5:503, 2021.
  - 35 Julian Wechs, Hippolyte Dourdent, Alastair A. Abbott, and Cyril Branciard. Quantum circuits with classical versus quantum control of causal order. *PRX Quantum*, 2:030335, August 2021. [doi:10.1103/PRXQuantum.2.030335](#).
  - 36 Matt Wilson and Giulio Chiribella. A diagrammatic approach to information transmission in generalised switches. *Electronic Proceedings in Theoretical Computer Science*, 340:333–348, September 2021. [doi:10.4204/eptcs.340.17](#).
  - 37 Mingsheng Ying, Nengkun Yu, and Yuan Feng. Defining quantum control flow. *arXiv preprint arXiv:1209.4379*, 2012.
  - 38 Magdalena Zych, Fabio Costa, Igor Pikovski, and Časlav Brukner. Bell’s theorem for temporal order. *Nature communications*, 10(1):1–10, 2019.

## A Proofs

### A.1 Proof of Proposition 5

Since there exists an orthonormal basis of  $\mathbb{C}^{[a]} \otimes \mathcal{V}$  composed of vectors of the form  $|c, p\rangle \otimes |\varphi\rangle$ , it suffices to check that  $V_D$  preserves all scalar products of vectors of this form. For any  $c, p, c', p', |\varphi\rangle$  and  $|\varphi'\rangle$ , one has  $(\langle c, p| \otimes \langle \varphi|) V_D^\dagger V_D (|c', p'\rangle \otimes |\varphi'\rangle) = \langle c_{c,p}^D, p_{c,p}^D | c_{c',p'}^D, p_{c',p'}^D \rangle \otimes \langle \varphi | U_{c,p}^{D\dagger} U_{c',p'}^D | \varphi' \rangle$ . On the one hand, it can be proved in the same way as in [13] that the function  $(c, p) \mapsto (c_{c,p}^D, p_{c,p}^D)$  is a bijection, so that  $(c_{c,p}^D, p_{c,p}^D) = (c_{c',p'}^D, p_{c',p'}^D)$  if and only if  $(c, p) = (c', p')$ . That is,  $\langle c_{c,p}^D, p_{c,p}^D | c_{c',p'}^D, p_{c',p'}^D \rangle = \langle c, p | c', p' \rangle = \begin{cases} 1 & \text{if } (c, p) = (c', p') \\ 0 & \text{if } (c, p) \neq (c', p') \end{cases}$ . On the

other hand, since  $U_{c,p}^D$  is an isometry, if  $(c, p) = (c', p')$  then  $\langle \varphi | U_{c,p}^{D\dagger} U_{c,p}^D | \varphi' \rangle = \langle \varphi | \varphi' \rangle$ . Thus,

$$\langle\langle c, p \mid \otimes \langle \varphi \mid V_D^\dagger V_D \mid \langle c', p' \rangle \otimes \mid \varphi' \rangle\rangle = \begin{cases} \langle \varphi \mid \varphi' \rangle & \text{if } (c, p) = (c', p') \\ 0 & \text{if } (c, p) \neq (c', p') \end{cases} = \langle\langle c, p \mid \otimes \langle \varphi \mid \mid \langle c', p' \rangle \otimes \mid \varphi' \rangle\rangle.$$

## A.2 Proof of Proposition 6

Let us assume that  $\mathbb{M}$  is a monoid of linear maps on a complex vector space  $\mathcal{V}$ .

Since the quantum semantics is defined from the action semantics, it is clear that  $\forall D, D', \llbracket D \rrbracket = \llbracket D' \rrbracket \Rightarrow V_D = V_{D'}$ .

Given an  $\mathbb{M}$ -diagram  $D$ , if  $0 \notin \mathbb{M}$ , then for all  $c, p$ ,  $U_{c,p}^D \neq 0$ , so that there exists  $\mid \varphi \rangle \in \mathcal{V}$  such that  $U_{c,p}^D \mid \varphi \rangle \neq 0$ . Then  $\mid c_{c,p}^D, p_{c,p}^D \rangle \otimes U_{c,p}^D \mid \varphi \rangle \neq 0$ , which implies that  $c_{c,p}^D$  and  $p_{c,p}^D$  are uniquely determined from the data of  $c, p$  and  $V_D$ . Since in any case,  $U_{c,p}^D$  is uniquely determined from the data of  $c, p$  and  $V_D$ , this implies that if  $0 \notin \mathbb{M}$  then  $\llbracket D \rrbracket$  is uniquely determined from  $V_D$ . Hence if  $0 \notin \mathbb{M}$  then for any two  $\mathbb{M}$ -diagrams  $D$  and  $D'$ ,  $V_D = V_{D'} \Rightarrow \llbracket D \rrbracket = \llbracket D' \rrbracket$ .

Conversely, if  $0 \in \mathbb{M}$ , then for example, with  $D = \text{---}\boxed{0}\text{---}$  and  $D' = \text{---}\boxed{0}\text{---}\text{---}\ominus\text{---}$ , both of type  $\top \rightarrow \top$ , one has  $V_D = V_{D'} = 0$  but  $\llbracket D \rrbracket(\mathbf{V}, 0) = ((\mathbf{V}, 0), 0) \neq \llbracket D' \rrbracket(\mathbf{V}, 0) = ((\mathbf{H}, 0), 0)$ .

## A.3 Proof of Propositions 11 and 10

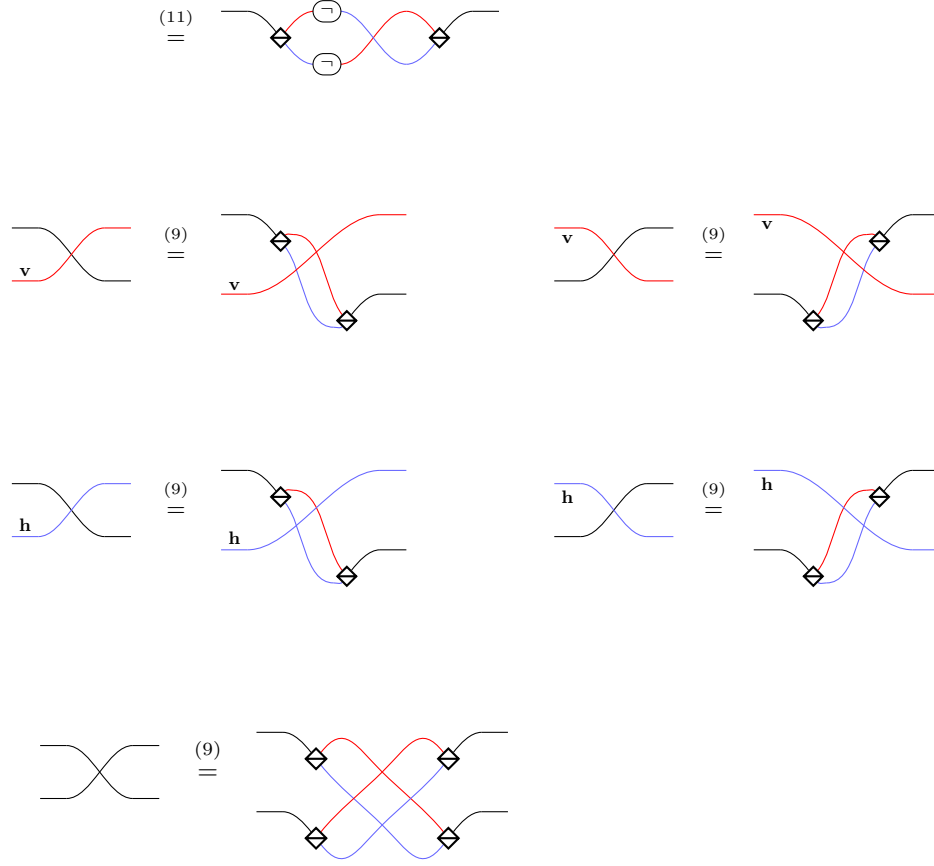
Given a monoid homomorphism  $\gamma: \mathcal{G}^* \rightarrow \mathcal{U}(\mathcal{H})$ , a  $\mathcal{G}^*$ -diagram  $D$  and any  $c, p$ , one has  $\llbracket \gamma(D) \rrbracket(c, p) = ((c_{c,p}^D, p_{c,p}^D), \gamma(w_{c,p}^D))$ . Therefore, to prove that  $\forall D_1, D_2, \llbracket \gamma(D_1) \rrbracket = \llbracket \gamma(D_2) \rrbracket \Rightarrow \llbracket D_1 \rrbracket = \llbracket D_2 \rrbracket$ , it suffices to prove that for any two words  $w_1, w_2 \in \mathcal{G}^*$ , if  $\gamma(w_1) = \gamma(w_2)$  then  $w_1 = w_2$ .

We first prove Proposition 11.

By Zorn's lemma, there exists a maximal family  $(\alpha_i)_{i \in I}$  of  $\mathbb{Q}$ -algebraically independent complex numbers of absolute value 1. Such a family must have the cardinality of  $\mathbb{C}$  (that is,  $2^{\aleph_0}$ ). Indeed, the cardinality of the set of polynomials in one variable with coefficients in the field extension of  $\mathbb{Q}$  generated by the  $\alpha_i$ , is  $\max(\aleph_0, \text{card}(I))$ , and since each of these polynomials has finitely many roots, the set of their roots has cardinality at most  $\max(\aleph_0, \text{card}(I))$ . If  $\text{card}(I)$  is strictly less than  $2^{\aleph_0}$ , then so is  $\max(\aleph_0, \text{card}(I))$ ; therefore, since the set  $\{\alpha \in \mathbb{C} \mid |\alpha| = 1\}$  has cardinality  $2^{\aleph_0}$ , it contains an element  $\alpha_\perp$  which is not a root of any of these polynomials, so that by adding  $\alpha_\perp$  to the family  $(\alpha_i)_{i \in I}$ , we still have a family of  $\mathbb{Q}$ -algebraically independent complex numbers of absolute value 1, which contradicts the maximality of  $(\alpha_i)_{i \in I}$ .

If the cardinality of  $\mathcal{G}$  is no greater than  $2^{\aleph_0}$ , then without loss of generality, we can assume that  $\mathcal{G} \subseteq I$ . We start with the case where  $\mathcal{H} = \mathbb{C}^2$ . We consider the function  $\gamma: U \in \mathcal{G} \mapsto H \begin{pmatrix} 1 & 0 \\ 0 & \alpha_U \end{pmatrix}$ , extended into a monoid homomorphism  $\gamma: \mathcal{G}^* \rightarrow \mathcal{U}(\mathbb{C}^2)$  (where  $H = \frac{1}{\sqrt{2}} \begin{pmatrix} 1 & 1 \\ 1 & -1 \end{pmatrix}$ ). Given two words  $w_1, w_2 \in \mathcal{G}^*$  such that  $w_1 \neq w_2$ , the entries of  $\gamma(w_1)$  and  $\gamma(w_2)$  are polynomials in the  $\alpha_U$  with coefficients in  $\mathbb{Q}$ . The two matrices of polynomials obtained by replacing each  $\alpha_U$  by a variable  $X_U$  in  $\gamma(w_1)$  and  $\gamma(w_2)$  differ by at least one entry: indeed, by instantiating each variable  $X_U$  by either  $e^{i\pi/4}$  or  $e^{3i\pi/4}$  in such a way that the sequence of angles induced by  $w_1$  and  $w_2$  are different, we get two different sequences of the patterns  $HT$  and  $HTS$  with  $T = \begin{pmatrix} 1 & 0 \\ 0 & e^{i\pi/4} \end{pmatrix}$  and  $S = T^2$ , and it follows from Theorem





- If  $D = D_1 \oplus D_2$ , then by induction hypothesis there exist two diagrams in normal form  $N_1$  and  $N_2$  such that  $\text{CPBS} \vdash D_1 = N_1$  and  $\text{CPBS} \vdash D_2 = N_2$ . Then  $\text{CPBS} \vdash D = N_1 \oplus N_2$  and it is easy to see that  $N_1 \oplus N_2$  is in normal form.
- If  $D = D_2 \circ D_1$ , then by induction hypothesis, let  $N_1$  and  $N_2$  be two diagrams in normal form such that  $\text{CPBS} \vdash D_1 = N_1$  and  $\text{CPBS} \vdash D_2 = N_2$ . Let us decompose them as  $N_1 = M_1 \circ P_1 \circ F_1 \circ G_1 \circ S_1$  and  $N_2 = M_2 \circ P_2 \circ F_2 \circ G_2 \circ S_2$ , following Definition 15. One has  $\text{CPBS} \vdash D = N_2 \circ N_1 = M_2 \circ P_2 \circ F_2 \circ G_2 \circ S_2 \circ M_1 \circ P_1 \circ F_1 \circ G_1 \circ S_1$ . Equation (10) makes  $S_2 \circ M_1$  equal to a parallel composition of red and blue identity wires, so that  $\text{CPBS} \vdash D = M_2 \circ P_2 \circ F_2 \circ G_2 \circ P_1 \circ F_1 \circ G_1 \circ S_1$ . By naturality of the swap, one has  $G_2 \circ P_1 = P_1 \circ G'_2$ , where  $G'_2$  is a parallel composition of coloured non-identity gates and identity wires, obtained by permuting the “rows” of  $G_2$ . One has (3), (25)  $\vdash G'_2 \circ F_1 = F_1 \circ G''_2$ , where  $G''_2$  is obtained by changing some colours in  $G'_2$ , and Equation (25) is the following variant of Equation (3):

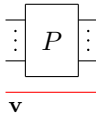
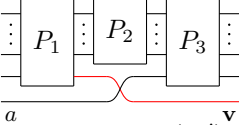
$$\text{h} \boxed{U} \text{---} \ominus \text{---} = \text{h} \ominus \text{---} \boxed{U} \text{---} \quad (25)$$

which is derived from the equations of Figure 4 as follows:

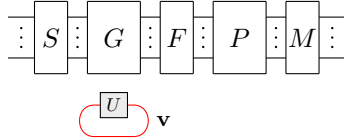
$$\begin{aligned} \text{h} \ominus \text{---} \boxed{U} \text{---} &\stackrel{(7)}{=} \text{h} \ominus \text{---} \boxed{U} \text{---} \ominus \text{---} \ominus \text{---} \\ &\stackrel{(3)}{=} \text{h} \ominus \text{---} \ominus \text{---} \boxed{U} \text{---} \ominus \text{---} \\ &\stackrel{(8)}{=} \text{h} \boxed{U} \text{---} \ominus \text{---} \end{aligned}$$

Thus,  $\text{CPBS} \vdash D = M_2 \circ P_2 \circ F_2 \circ P_1 \circ F_1 \circ G_2'' \circ G_1 \circ S_1$ . By naturality of the swap, one has  $F_2 \circ P_1 = P_1 \circ F_2'$ , where  $F_2'$  is a parallel composition of coloured identities and negations (obtained by permuting  $F_2$ ). One has  $(7), (8) \vdash F_2' \circ F_1 = F''$ , where  $F''$  is obtained by removing all double negations in  $F_2' \circ F_1$ . Finally,  $(2), (1) \vdash G_2'' \circ G_1 = G'''$ , where  $G'''$  is still a parallel composition of coloured non-identity gates and identity wires. Thus,  $\text{CPBS} \vdash D = M_2 \circ (P_2 \circ P_1) \circ F'' \circ G''' \circ S_1$ , with  $S_1, G''', F'', (P_2 \circ P_1)$  and  $M_2$  respectively of the forms described in Definition 15, so that their composition is in normal form. This gives us the result.

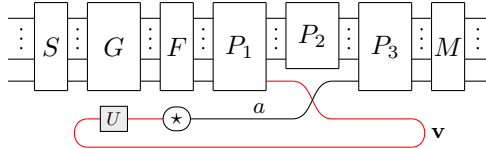
- If  $D = \text{Tr}_{\mathbf{v}}(D') : a \rightarrow b$ , then by induction hypothesis, let  $N'$  be a diagram in normal form such that  $\text{CPBS} \vdash D' = N'$ . Let us decompose it as  $N' = M' \circ P' \circ F' \circ G' \circ S'$ , following Definition 15. Since  $N'$  is of type  $a \oplus \mathbf{v} \rightarrow b \oplus \mathbf{v}$ ,  $S'$  (resp.  $M'$ ) is of the form  $S \oplus \overline{\mathbf{v}}$  (resp.  $M \oplus \overline{\mathbf{v}}$ ) where  $S$  (resp.  $M$ ) is a parallel composition of coloured identity wires and copies of  $\overline{\text{box}} \overline{\text{box}}$  (resp.  $\overline{\text{box}} \overline{\text{box}}$ ). Using the structural congruence, one

can write  $P'$  in the form  or , where  $P$ , or  $P_1, P_2$  and  $P_3$ ,

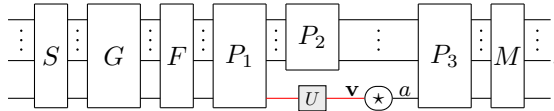
are permutations of the wires. In the first case,  $\text{Tr}_{\mathbf{v}}(N')$  can (still using the structural congruence) be written in the form



with  $S, G, F, P$  and  $M$  of the forms demanded by Definition 15 (in particular,  $F'$  cannot have a negation on its bottom wire since this would prevent  $N'$  from being of type  $a \oplus \mathbf{v} \rightarrow b \oplus \mathbf{v}$ ), so that  $(6) \vdash \text{Tr}_{\mathbf{v}}(N') = \overline{\text{box}} \overline{\text{box}} \overline{\text{box}} \overline{\text{box}} \overline{\text{box}}$ , which is in normal form. In the second case,  $\text{Tr}_{\mathbf{v}}(N')$  can be written in the form



where  $\overline{\text{box}} \overline{\text{box}} \overline{\text{box}}$  is either  $\overline{\text{box}} \overline{\text{box}}$  or  $\overline{\text{box}} \overline{\text{box}}$ . Then using the structural congruence (in particular the yanking axiom), one can write it in the form



By naturality of the swap, one can slide the gate  $U$  and the possible negation through  $P_1$ . Then, possibly using Equation (25), one can move the gate  $U$  to the other side of  $F$ . Finally, it may remain to merge  $U$  with a gate of  $G$  using Equation (2) or its following variant:

$$\overline{\text{box}} \overline{\text{box}} \overline{\text{box}} = \overline{\text{box}} \overline{\text{box}} \overline{\text{box}} \quad (26)$$

and/or to remove a double negation using Equation (8). Then one gets a diagram in normal form.

Equation (26) is derived from the equations of Figure 4 as follows:

$$\begin{aligned}
\mathbf{h} \text{---} \boxed{U} \text{---} \boxed{V} \text{---} &\stackrel{(8)(3)}{=} \mathbf{h} \text{---} \ominus \text{---} \boxed{U} \text{---} \boxed{V} \text{---} \ominus \text{---} \\
&\stackrel{(2)}{=} \mathbf{h} \text{---} \ominus \text{---} \boxed{VU} \text{---} \ominus \text{---} \\
&\stackrel{(3)(8)}{=} \mathbf{h} \text{---} \boxed{VU} \text{---}
\end{aligned}$$

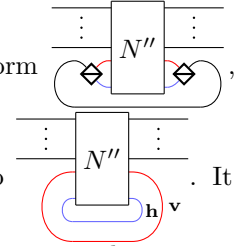
- The case  $D = Tr_{\mathbf{h}}(D') : a \rightarrow b$  is analogous to the previous case. Instead of using Equations (3) and (6), one uses respectively Equation (25) and the following variant of Equation (6):

$$\boxed{U} \text{---} \mathbf{h} = \boxed{\phantom{U}} \tag{27}$$

which is derived from the equations of Figure 4 as follows:

$$\begin{aligned}
\boxed{U} \text{---} \mathbf{h} &\stackrel{(8)}{=} \boxed{U} \text{---} \ominus \text{---} \ominus \text{---} \mathbf{h} \\
&= \ominus \text{---} \boxed{U} \text{---} \ominus \text{---} \mathbf{v} \\
&\stackrel{(3)}{=} \boxed{U} \text{---} \ominus \text{---} \ominus \text{---} \mathbf{v} \\
&\stackrel{(7)}{=} \boxed{U} \text{---} \mathbf{v} \\
&\stackrel{(6)}{=} \boxed{\phantom{U}}
\end{aligned}$$

- If  $D = Tr_{\top}(D') : a \rightarrow b$ , then by induction hypothesis, let  $N'$  be a diagram in normal form such that  $CPBS \vdash D' = N'$ .  $Tr_{\top}(N')$  can be written in the form



which by dinaturality and Equation (10), can be transformed into

suffices then to proceed successively as in the two preceding cases to get a diagram in normal form.

## A.5 Proof of Lemma 17

If  $\llbracket N \rrbracket = \llbracket N' \rrbracket$ , then in particular  $N$  and  $N'$  have same type:  $N, N' : a \rightarrow b$  for some  $a, b$ .

Let us decompose  $N$  and  $N'$  into  $N = M \circ P \circ F \circ G \circ S$  and  $N' = M' \circ P' \circ F' \circ G' \circ S'$ .

It follows directly from the definition that  $S$  and  $S'$  are uniquely determined by their input type, so that since they both have input type  $a$ ,  $S = S'$ . Similarly,  $M$  and  $M'$  are uniquely determined by their output type, so that since they both have output type  $b$ ,  $M = M'$ .

Let  $S^{-1}$  and  $M^{-1}$  be the horizontal reflections of respectively  $S$  and  $M$ , that is, the diagrams obtained by replacing  $\overleftarrow{\diamond}$  by  $\overrightarrow{\diamond}$  in  $S$  and  $\overleftarrow{\diamond}$  by  $\overrightarrow{\diamond}$  in  $M$ . One has (10)  $\vdash M^{-1} \circ N \circ S^{-1} = P \circ F \circ G$  and (10)  $\vdash M^{-1} \circ N' \circ S^{-1} = P' \circ F' \circ G'$ , so that by Proposition 14,



$\llbracket M^{-1} \circ N \circ S^{-1} \rrbracket = \llbracket P \circ F \circ G \rrbracket = \llbracket M^{-1} \circ N' \circ S^{-1} \rrbracket = \llbracket P' \circ F' \circ G' \rrbracket$ . For any  $c, p$ , one has  $\llbracket P \circ F \circ G \rrbracket(c, p) = ((c_{c,p}^F, p_{c,p}^P), U_{c,p}^G)$  and  $\llbracket P' \circ F' \circ G' \rrbracket(c, p) = ((c_{c,p}^{F'}, p_{c,p}^{P'}), U_{c,p}^{G'})$ , so that  $U_{c,p}^G = U_{c,p}^{G'}$ ,  $c_{c,p}^F = c_{c,p}^{F'}$  and  $p_{c,p}^P = p_{c,p}^{P'}$ . Because of their respective forms required by Definition 15,  $G, G', F, F', P$  and  $P'$  are uniquely determined by the family of, respectively, the  $U_{c,p}^G$ , the  $U_{c,p}^{G'}$ , the  $c_{c,p}^F$ , the  $c_{c,p}^{F'}$ , the  $p_{c,p}^P$ , and the  $p_{c,p}^{P'}$ . Hence,  $G = G', F = F'$  and  $P = P'$ .

## A.6 Proof of Theorem 19

For

- each of Equations (1), (4), and (7)–(17)
- each instance of Equations (3) and (5)
- the class of all instances of Equation (2) without  $I$  gates in the left-hand side
- each class of instances of Equation (6) given by an equivalence class of elements of  $\mathbf{M}$  for the equivalence relation  $\sim_{\text{conj}}^*$ , defined as the transitive closure of  $\sim_{\text{conj}}$ , itself defined by  $U \sim_{\text{conj}} V$  if there exist  $W, T \in \mathbf{M}$  such that  $U = WT$  and  $V = TW$

we give an invariant that is satisfied by exactly one side of the considered equation (or of each element of the considered class of instances of Equation (2) or (6)), and such that for any diagram  $D$ , applying any other equation or instance inside  $D$  (that is, replacing a sub-diagram of  $D$  that matches one side of the equation by the other side) preserves the fact that  $D$  satisfies the invariant or not. In each case, this proves that the equations that break the invariant are not consequences of those that preserve it in any diagram.

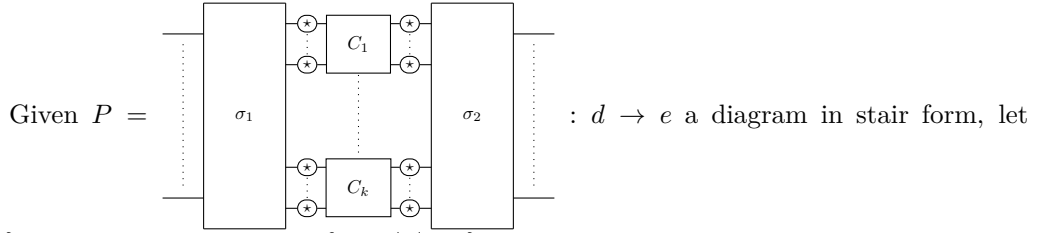
Note that the instances of Equation (2) with an  $I$  gate in the left-hand side are consequences of Equation (1), and that the elements of a class of instances of Equation (6) are consequences of any particular instance of Equation (6) of the same class together with Equation (2).

- For Equation (1), the invariant is that at least one gate can be reached by a particle from an input wire.
- For the class of all instances of Equation (2) without  $I$  gates in the left-hand side, the invariant is the maximum number of non- $I$  gates that a particle coming from an input wire can traverse along its path in the diagram.
- For each instance of Equation (3) given by a particular  $U$ , the invariant is that all gates labelled with  $U$  are red.
- For Equation (4), the invariant is that the diagram contains a (black)  $-\text{⊖}-$ .
- For each instance of Equation (5) given by a particular  $U$ , the invariant is that the diagram contains a (black)  $-\text{⊔}-$ .
- For each class of instances of Equation (6), the invariant is that there exists a wire in the diagram and a polarisation  $\mathbf{V}$  or  $\mathbf{H}$  such that the path of a particle starting from this wire with this polarisation is a closed loop, and that the product of the labels of the gates traversed by the particle before getting back to its starting point with its initial polarisation for the first time, is an element of the equivalence class (note that this does not depend on the choice of the starting point).
- For Equation (7), the invariant is that all wires are red.
- For Equation (8), the invariant is that no particle entering the diagram by a blue input wire can reach the output without passing through a negation at some point in the diagram. Note that Equation (7) cannot change this invariant because in order to reach a red wire, the particle coming from a blue wire has to get its polarisation changed, and therefore to pass through a negation.

- For Equation (9), the invariant is that all wires are black and the diagram is non-empty and does not contain any  $\overline{\text{X}}$ .
- For Equation (10), the invariant is that the diagram contains at least one black wire.
- For Equation (11), the invariant is that the diagram contains at least one generator among  $\overline{\text{X}}$ ,  $\overline{\text{Y}}$ ,  $\overline{\text{V}}$ ,  $\overline{\text{H}}$  and  $\overline{\text{C}}$ .
- For Equation (12), the invariant is that the diagram contains at least one generator among  $\overline{\text{X}}$ ,  $\overline{\text{Y}}$ ,  $\overline{\text{V}}$  and  $\overline{\text{H}}$ .
- For Equation (13), the invariant is that the diagram contains a  $\overline{\text{X}}$ .
- For Equation (14), the invariant is that the diagram contains a  $\overline{\text{V}}$ .
- For Equation (15), the invariant is that the diagram contains a  $\overline{\text{H}}$ .
- For Equation (16), the invariant is that the diagram contains a  $\overline{\text{X}}$ .
- For Equation (17), the invariant is that the diagram contains a  $\overline{\text{H}}$ .

## A.7 Proof of Theorem 27

Given any gate-free diagram  $Q : d \rightarrow e$ , we denote by  $\{d_i^Q\}_{i=1,\dots,k_Q}$  the finest partition of  $\{0, \dots, |d| - 1\}$  such that there exists a partition  $\{e_i^Q\}_{i=1,\dots,k_Q}$  of  $\{0, \dots, |e| - 1\}$  satisfying  $\forall i, \forall c, p, (p \in d_i^Q \Leftrightarrow p_{c,p}^P \in e_i^Q)$ . It is easy to see that the partition  $\{e_i^Q\}_{i=1,\dots,k_Q}$  is unique and that symmetrically, it is the finest partition of  $\{0, \dots, |e| - 1\}$  such that there exists a partition  $\{f_i^Q\}_{i=1,\dots,k_Q}$  of  $\{0, \dots, |d| - 1\}$  satisfying  $\forall i, \forall c, p, (p \in f_i^Q \Leftrightarrow p_{c,p}^P \in e_i^Q)$  (which of course implies that  $\forall i, f_i^Q = d_i^Q$ ).



$\{d_i\}_{i=1,\dots,k}$  be the partition of  $\{0, \dots, |d| - 1\}$  such that an index  $j$  is in  $d_i$  if the input wire of  $P$  of index  $j$  is connected to  $C_i$ . Similarly, let  $\{e_i\}_{i=1,\dots,k}$  be the partition of  $\{0, \dots, |e| - 1\}$  such that an index  $j$  is in  $e_i$  if the output wire of  $P$  of index  $j$  is connected to  $C_i$ . One has  $\forall i, \forall c, p, (p \in d_i \Leftrightarrow p_{c,p}^P \in e_i)$ . It is easy to see that  $\{d_i\}_{i=1,\dots,k}$  is the finest partition of  $\{0, \dots, |d| - 1\}$  such that there exists  $\{e_i\}_{i=1,\dots,k}$  satisfying this property, that is, up to reordering the partitions, one has  $k = k_P$  and  $\forall i, d_i = d_i^P$  and  $e_i = e_i^P$ .

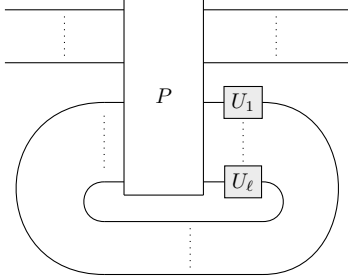
Again given an arbitrary gate-free diagram  $Q : d \rightarrow e$ , let us decompose  $d = x_1 \oplus \dots \oplus x_n$  and  $e = y_1 \oplus \dots \oplus y_m$ , with  $\forall j, x_j, y_j \in \{\mathbf{v}, \mathbf{h}, \top\}$ . Since any gate-free diagram is equivalent to a diagram in stair form (indeed, by applying Steps 2 to 7 of the PGT procedure described below — which does not rely on Theorem 27 — one can put any gate-free diagram in stair form), the preceding paragraph, because of the input/output types of the five kinds of staircases, implies that for every  $i$  there are four cases:

1.  $|d_i^Q| = |e_i^Q|$ ,  $\forall j \in d_i^Q, x_j = \top$  and  $\forall j \in e_i^Q, y_j = \top$
2.  $|d_i^Q| = |e_i^Q|$  and exactly one element of  $d_i^Q$  and one element of  $e_i^Q$  are not equal to  $\top$
3.  $|d_i^Q| = |e_i^Q| + 1$ ,  $\forall j \in e_i^Q, y_j = \top$  and exactly two elements of  $d_i^Q$  are not equal to  $\top$
4.  $|e_i^Q| = |d_i^Q| + 1$ ,  $\forall j \in d_i^Q, x_j = \top$  and exactly two elements of  $e_i^Q$  are not equal to  $\top$



### A.8 Proof of Theorem 31

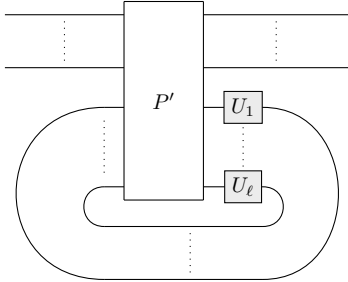
Let  $D_1 : a \rightarrow b$  be an abstract diagram obtained from applying the query optimisation procedure followed by the PGT procedure, in which all gates bear different labels. We write it in the form



with  $P$  in stair form and  $U_1, \dots, U_\ell \in \mathcal{G}$  (where all wires and gates can be of arbitrary colours).

For each  $(c, p) \in [a]$ , let  $p_{c,p}^{(1)}, \dots, p_{c,p}^{(\ell_{c,p})}$  be the sequence of positions such that  $w_{c,p}^{D_1} = U_{p_{c,p}^{(1)}} \dots U_{p_{c,p}^{(\ell_{c,p})}}$  (with  $\ell_{c,p} = |w_{c,p}^{D_1}|$ ). This sequence is determined without ambiguity since the names  $U_i$  are pairwise distinct. There exists a sequence of polarisations  $c_{c,p}^{(1)}, \dots, c_{c,p}^{(\ell_{c,p})}$  such that  $\llbracket P \rrbracket(c, p) = ((c_{c,p}^{(1)}, |b| + p_{c,p}^{(1)}), \epsilon)$ ,  $\forall i \in \{1, \dots, \ell_{c,p} - 1\}$ ,  $\llbracket P \rrbracket(c_{c,p}^{(i)}, |a| + p_{c,p}^{(i)}) = ((c_{c,p}^{(i+1)}, |b| + p_{c,p}^{(i+1)}), \epsilon)$ , and  $\llbracket P \rrbracket(c_{c,p}^{(\ell_{c,p})}, |a| + p_{c,p}^{(\ell_{c,p})}) = ((c_{c,p}^{D_1}, p_{c,p}^{D_1}), \epsilon)$  (where  $\epsilon$  denotes the empty word).

Given a query-PBS-optimal diagram  $D'_1$  equivalent to  $D_1$ , up to applying the query optimisation procedure and the PGT procedure, we can assume that  $D'_1$  is in PGT form. Note that any diagram  $E$  obtained from applying the query optimisation procedure necessarily satisfies that, for every  $U \in \mathcal{G}$ , it contains exactly  $\left\lfloor \sum_{(c,p) \in [a]} \frac{|w_{c,p}^E| |U|}{2} \right\rfloor$  black gates labelled with  $U$ , and one red or blue gate labelled with  $U$  if and only if  $\sum_{(c,p) \in [a]} |w_{c,p}^E| |U|$  is odd. Since the PGT procedure does not change the gates, it preserves this property. Therefore,  $D_1$  and  $D'_1$  both satisfy this property, and since they have the same semantics, this implies that they have the same gates up to turning some red gates into blue gates and vice-versa. That is, up to slightly deforming it in order to permute the gates, we can put  $D'_1$  in the form

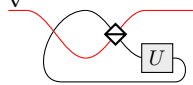
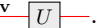


with  $P'$  in stair form. For each  $(c, p) \in [a]$ , there also exists a sequence of polarisations  $c'_{c,p}{}^{(1)}, \dots, c'_{c,p}{}^{(\ell_{c,p})}$  such that  $\llbracket P' \rrbracket(c, p) = ((c'_{c,p}{}^{(1)}, |b| + p_{c,p}^{(1)}), \epsilon)$ ,  $\forall i \in \{1, \dots, \ell_{c,p} - 1\}$ ,  $\llbracket P' \rrbracket(c'_{c,p}{}^{(i)}, |a| + p_{c,p}^{(i)}) = ((c'_{c,p}{}^{(i+1)}, |b| + p_{c,p}^{(i+1)}), \epsilon)$ , and  $\llbracket P' \rrbracket(c'_{c,p}{}^{(\ell_{c,p})}, |a| + p_{c,p}^{(\ell_{c,p})}) = ((c_{c,p}^{D_1}, p_{c,p}^{D_1}), \epsilon)$ .

Let  $P''$  be the diagram obtained from  $P'$  by adding, for every position  $q$  such that there exist  $c, p$  and  $i \in \{1, \dots, \ell_{c,p}\}$  satisfying  $q = p_{c,p}^{(i)}$  and  $c_{c,p}^{(i)} \neq c'_{c,p}{}^{(i)}$ , a negation on input wire  $|a| + q$  and on output wire  $|b| + q$ . Let  $d$  be such that  $P : a \oplus d \rightarrow b \oplus d$ . It is easy to see that for every  $(c, p) \in [a]$ , and for every couple  $(c, p) \in [a \oplus d]$  with  $p \geq |a|$  that can be written as  $(c'_{c',p'}{}^{(i)}, |a| + p_{c',p'}{}^{(i)})$  for some  $c', p' \in [a]$  and  $i \in \{1, \dots, \ell_{c',p'}\}$ , one has  $\llbracket P'' \rrbracket(c, p) = \llbracket P \rrbracket(c, p)$ . Since  $D_1$  is query-optimal, every black gate can be reached from two basis states  $(c, p) \in [a]$

and every non-black gate can be reached from one basis state, which implies that every couple  $(c, p) \in [b \oplus d]$  with  $p \geq |b|$  can be written as  $(c_{c', p'}^{(i)}, |b| + p_{c', p'}^{(i)})$ , and therefore, every couple  $(c, p) \in [a \oplus d]$  with  $p \geq |a|$  can be written as  $(c_{c', p'}^{(i)}, |a| + p_{c', p'}^{(i)})$ . Hence,  $P''$  has the same semantics as  $P$ . Since by construction,  $P''$  contains the same number of PBS as  $P'$ , and by Theorem 27,  $P$  is PBS-optimal, this implies that  $P$  contains at most as many PBS as  $P'$ , that is,  $D_1$  contains at most as many PBS as  $D'_1$ . Hence,  $D_1$  is query-PBS-optimal.

► **Remark 38.** The proof of Theorem 31 uses the fact that the diagrams output by the query optimisation procedure, in addition of being query-optimal, have the property that if a gate is used only once (that is, if it is accessible from only one input state  $(c, p)$ , and a particle with this input state traverses only once the gate), then it is represented as red or blue. Note that a diagram in PGT form with only one query to each oracle may not be query-PBS-optimal if

it contains a black gate used only once. For instance,  is in PGT form but not query-PBS-optimal as it is equivalent to .

## A.9 NP-Hardness Results

### A.9.1 Proof of Theorem 32

Let  $\mathcal{G}$  be a set of names. We will prove that the problem is already NP-hard when we restrict the input diagram to the family  $\mathcal{P}$  defined as follows:

► **Definition 39.** Given a word  $w = w_0 \dots w_{n-1}$  with  $w_0, \dots, w_{n-1} \in \mathcal{G}$  and a permutation  $\sigma$  of  $[n]$ , we define  $\sigma(w)$  as the rearranged word  $w_{\sigma(0)} \dots w_{\sigma(n-1)}$ .

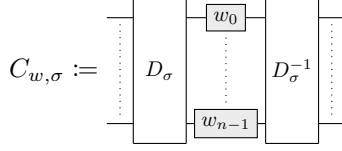
► **Definition 40.** We denote by  $\mathcal{P}$  the set of  $\mathcal{G}^*$ -diagrams  $D : \top^{\oplus n} \rightarrow \top^{\oplus n}$  such that there exists a word  $w = w_0 \dots w_{n-1} \in \mathcal{G}^n$  and a permutation  $\sigma$  of  $[n]$  such that for every  $p \in [n]$ ,  $\llbracket D \rrbracket(\mathbf{V}, p) = ((\mathbf{V}, p), w_p)$  and  $\llbracket D \rrbracket(\mathbf{H}, p) = ((\mathbf{H}, p), w_{\sigma(p)})$ .

We polynomially reduce this restricted problem from the *maximum Eulerian cycle decomposition problem*, also called MAX-ECD [9], which consists in, given an Eulerian undirected graph  $G$ , finding a maximum-cardinality edge-partition of  $G$  into cycles (that is, partitioning the set of edges of  $G$  into the maximum number of cycles). Note that the NP-hardness of MAX-ECD follows directly from the NP-completeness of the problem of deciding whether  $G$  can be edge-partitioned into triangles, which is proved in [26] (it corresponds to the case of the edge-partition into copies of the complete graph  $K_3$ ).

The MAX-ECD problem is equivalent to the problem of, given an Eulerian graph  $G$ , finding a suitable orientation of its edges together with an edge-partition of the resulting directed graph into directed cycles, so that the number of cycles is maximal among all possible choices of orientation and partition. Indeed, given these, it suffices to erase the directions of the edges to get an undirected edge-partition into cycles, and given such a partition, it suffices to choose, for each cycle, one of the two possible ways of orienting it.

Given an Eulerian graph  $G$ , we construct a diagram of  $\mathcal{P}$  as follows: first, we choose an arbitrary orientation of the edges of  $G$  so as to get an Eulerian directed graph  $\vec{G}$  (which can be done by following an Eulerian circuit of  $G$ , which itself can be found in polynomial time [21]) and we associate a label, more precisely an element of  $\mathcal{G}$ , with each vertex of  $G$ , in such a way that any two distinct vertices bear distinct labels. Without loss of generality, we can assume that the vertices of  $G$  are elements of  $\mathcal{G}$  and thereby identify them with their labels. We enumerate the edges of  $\vec{G}$  as  $e_0, \dots, e_{n-1}$ . In  $\vec{G}$  — since it is Eulerian — each vertex has in- and out-degree equal, that is, each vertex appears as many times as the head

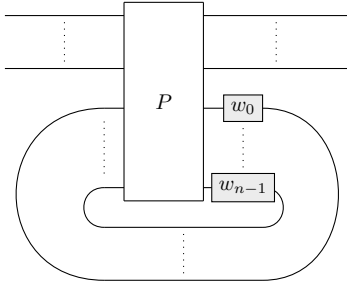
of an arrow as the tail of an arrow, hence there exists a permutation  $\sigma$  of  $[n]$  and a word  $w = w_0 \dots w_{n-1} \in \mathcal{G}^n$  such that for any  $p \in [n]$ ,  $e_p$  is of the form  $(w_p, w_{\sigma(p)})$ . We consider the following diagram:



where  $D_\sigma : \top^{\oplus n} \rightarrow \top^{\oplus n}$  is a  $\neg$ -free diagram in stair form<sup>7</sup> such that for any  $p \in [n]$ ,  $\llbracket D_\sigma \rrbracket (\mathbf{V}, p) = ((\mathbf{V}, p), \epsilon)$  and  $\llbracket D_\sigma \rrbracket (\mathbf{H}, p) = ((\mathbf{H}, \sigma(p)), \epsilon)$ , and  $D_\sigma^{-1}$  is the horizontal reflection of  $D_\sigma$ , which therefore satisfies that for any  $p \in [n]$ ,  $\llbracket D_\sigma^{-1} \rrbracket (\mathbf{V}, p) = ((\mathbf{V}, p), \epsilon)$  and  $\llbracket D_\sigma^{-1} \rrbracket (\mathbf{H}, p) = ((\mathbf{H}, \sigma^{-1}(p)), \epsilon)$ .

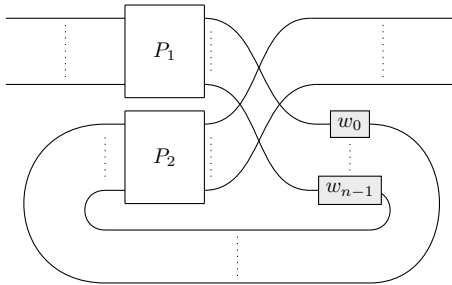
For any  $p \in [n]$ , one has  $\llbracket C_{w,\sigma} \rrbracket (\mathbf{V}, p) = ((\mathbf{V}, p), w_p)$  and  $\llbracket C_{w,\sigma} \rrbracket (\mathbf{H}, p) = ((\mathbf{H}, p), w_{\sigma(p)})$ . In particular,  $C_{w,\sigma}$  is in  $\mathcal{P}$ , and for any  $p \in [n]$ ,  $w_{\mathbf{V},p}^{C_{w,\sigma}}$  is the tail of  $e_p$  and  $w_{\mathbf{H},p}^{C_{w,\sigma}}$  is the head of  $e_p$ .<sup>8</sup>

Let  $C_{w,\sigma}^{\text{opt}}$  be a query-PBS-optimal diagram equivalent to  $C_{w,\sigma}$ . Up to applying the PGT procedure, which can be done in polynomial time and neither changes the gates nor increases the number of PBS, we can assume that  $C_{w,\sigma}^{\text{opt}}$  is in PGT form. That is, up to reordering some wires, it is of the form



with  $P$  in stair form. Since for every  $c, p$ , the word  $w_{c,p}^{C_{w,\sigma}^{\text{opt}}}$  has length 1,  $P$  is such that for any  $c \in \{\mathbf{V}, \mathbf{H}\}$  and  $p \in [n]$ , one has  $p_{c,p}^P \in \{n, \dots, 2n-1\}$  and  $p_{c,p+n}^P \in [n]$ .

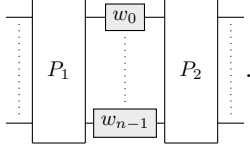
By looking at the semantics of a generic diagram in stair form (in particular by considering the functions  $\rho_i$  and  $\tau_i$  defined in the proof of Theorem 27), it is easy to see that this implies that up to reordering the wires on the sides of  $P$ , we can write  $C_{w,\sigma}^{\text{opt}}$  in the form



<sup>7</sup> Note that the type of  $D_\sigma$  forces all of its staircases to be made only of all-black PBS.

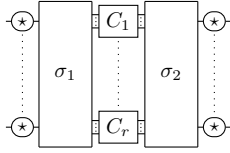
<sup>8</sup> See the end of Definition 2 for the definition of  $w_{c,p}^{C_{w,\sigma}}$ . Note that we identify words of length 1 with their single letter.

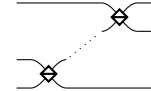
where  $P_1$  and  $P_2$  are two diagrams in stair form. Up to a few more deformations,  $C_{w,\sigma}^{\text{opt}}$  is of the form



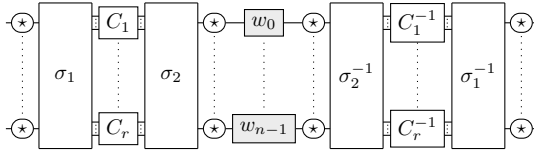
Due to the semantics of  $C_{w,\sigma}^{\text{opt}}$ , for any  $c, c' \in \{\mathbf{V}, \mathbf{H}\}$  and  $p, p' \in [n]$ , if  $\llbracket P_1 \rrbracket (c, p) = ((c', p'), \epsilon)$  then  $\llbracket P_2 \rrbracket (c', p') = ((c, p), \epsilon)$ . Hence, one can replace  $P_1$  or  $P_2$  by the horizontal reflection of the other without changing the semantics. This implies that  $P_1$  and  $P_2$  contain the same number of PBS (otherwise, by replacing the one with more PBS by the horizontal reflection of the other, one would obtain a diagram equivalent to  $C_{w,\sigma}^{\text{opt}}$  with strictly fewer PBS, which would contradict its query-PBS-optimality), and subsequently, that the diagram  $C_{w,\sigma}^{\text{opt}'}$  obtained by replacing  $P_2$  by the horizontal reflection  $P_1^{-1}$  of  $P_1$  is still query-PBS-optimal.

Up to slightly deforming  $P_1$ , we can write it in the form



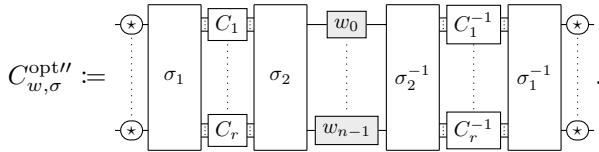
where  $\sigma_1$  and  $\sigma_2$  are permutations of the wires, the  $C_k$  are of the form , and

$\odot$  denotes either  $\text{---}$  or  $\ominus$ . Using this, we can write  $C_{w,\sigma}^{\text{opt}'}$  in the form

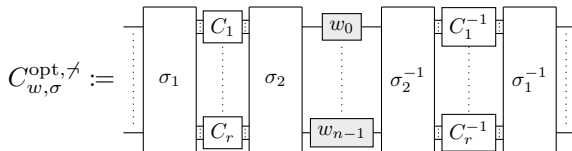


where given any gate-free diagram  $D$ ,  $D^{-1}$  denotes its horizontal reflection.

Since the diagram is symmetric, we can remove the negations in the middle without changing the semantics of the diagram or its query-PBS-optimality. This gives us



Let us consider the diagram



obtained by removing all negations on the sides of  $C_{w,\sigma}^{\text{opt}''}$ . For each  $p \in [n]$  such that there was a negation on the  $p$ th input and output wire, one now has  $\llbracket C_{w,\sigma}^{\text{opt},\gamma} \rrbracket (\mathbf{V}, p) = ((\mathbf{V}, p), w_{\sigma(p)})$  and  $\llbracket C_{w,\sigma}^{\text{opt},\gamma} \rrbracket (\mathbf{H}, p) = ((\mathbf{H}, p), w_p)$ . Let us consider the directed graph  $\tilde{G}$  obtained by

reversing the edge  $e_p$  in  $\vec{G}$  for every such  $p$ . For every  $p \in [n]$ , we denote by  $\tilde{e}_p$  the  $p$ th edge of  $\tilde{G}$ , which is either  $e_p$  or its reverse  $(w_{\sigma(p)}, w_p)$ . Then for every  $p \in [n]$ ,  $w_{\mathbf{V}, p}^{C_{w, \sigma}^{\text{opt}, \mathcal{A}'}}$  is the tail of  $\tilde{e}_p$  and  $w_{\mathbf{H}, p}^{C_{w, \sigma}^{\text{opt}, \mathcal{A}'}}$  is the head of  $\tilde{e}_p$ .

$\tilde{G}$  can be edge-partitioned into  $r$  cycles as follows: For each  $k \in \{1, \dots, r\}$ , let  $n_k$  be such that  $C_k : \top^{\oplus n_k} \rightarrow \top^{\oplus n_k}$ . Let also  $N_k := \sum_{j=1}^{k-1} n_j$ . By abuse of notation, we denote by  $\sigma_1$  and  $\sigma_2$  the permutations of  $[n]$  respectively associated with the diagrams  $\sigma_1$  and  $\sigma_2$ , so that  $\forall c, p, \llbracket \sigma_1 \rrbracket (c, p) = ((c, \sigma_1(p)), \epsilon)$  and  $\llbracket \sigma_2 \rrbracket (c, p) = ((c, \sigma_2(p)), \epsilon)$ . Note that for any  $k \in \{1, \dots, r\}$  and any  $p \in [n_k]$ , one has

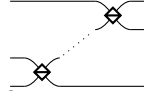
- $\forall i \in [n_k], \llbracket C_{w, \sigma}^{\text{opt}, \mathcal{A}'} \rrbracket (\mathbf{V}, \sigma_1^{-1}(N_k + i)) = ((\mathbf{V}, \sigma_1^{-1}(N_k + i)), w_{\sigma_2(N_k + i)})$
- $\forall i \in [n_k - 1], \llbracket C_{w, \sigma}^{\text{opt}, \mathcal{A}'} \rrbracket (\mathbf{H}, \sigma_1^{-1}(N_k + i)) = ((\mathbf{H}, \sigma_1^{-1}(N_k + i)), w_{\sigma_2(N_k + i + 1)})$
- $\llbracket C_{w, \sigma}^{\text{opt}, \mathcal{A}'} \rrbracket (\mathbf{H}, \sigma_1^{-1}(N_k + n_k - 1)) = ((\mathbf{H}, \sigma_1^{-1}(N_k + n_k - 1)), w_{\sigma_2(N_k)})$ .

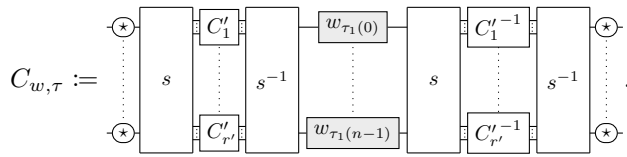
Hence, there is a cycle  $w_{\sigma_2(N_k)} \rightarrow w_{\sigma_2(N_k + 1)} \rightarrow \dots \rightarrow w_{\sigma_2(N_k + n_k - 1)} \rightarrow w_{\sigma_2(N_k)}$  in  $\tilde{G}$ , associated with  $C_k$ . Considering the cycle associated with each  $C_k$  gives us an edge-partition of  $\tilde{G}$  into  $r$  cycles, since these cycles are edge-disjoint and cover all edges of  $\tilde{G}$ .

It remains to prove that there is no orientation of the edges of  $G$  such that the resulting directed graph can be edge-partitioned into more than  $r$  cycles. Reasoning by contradiction, assume that there exists such an orientation yielding an Eulerian directed graph  $\tilde{G}$  with an edge-partition into  $r'$  cycles with  $r' > r$ . We enumerate these cycles in an arbitrary order, and denote by  $m_k$  the length of the  $k$ th cycle, for  $k \in \{1, \dots, r'\}$ . We denote by  $\tilde{e}_p$  the  $p$ th edge of  $\tilde{G}$ , which is either  $\tilde{e}_p$  or its reverse. Note that the in- and out-degree of each vertex are the same in  $\tilde{G}$  as in  $\vec{G}$  and  $\tilde{G}$ , so that there exist two permutations  $\tau_1$  and  $\tau_2$  of  $[n]$  such that  $\forall p \in [n], \tilde{e}_p = (w_{\tau_1(p)}, w_{\tau_2(p)})$ . Therefore, there exists an enumeration of  $[n]$  as  $(i_\ell^k)_{k \in \{1, \dots, r'\}, \ell \in [m_k]}$ , such that the  $k$ th cycle can be written

$$w_{\tau_1(i_0^k)} \xrightarrow{\tilde{e}_{i_0^k}} w_{\tau_1(i_1^k)} \xrightarrow{\tilde{e}_{i_1^k}} \dots \xrightarrow{\tilde{e}_{i_{m_k-2}^k}} w_{\tau_1(i_{m_k-1}^k)} \xrightarrow{\tilde{e}_{i_{m_k-1}^k}} w_{\tau_1(i_0^k)}.$$

Let  $s$  be the permutation of  $[n]$  such that  $\forall k, \ell, s(i_\ell^k) = M_k + \ell$ , where  $M_k := \sum_{j=1}^{k-1} m_j$ . We make the same abuse of notation as for  $\sigma_1$  and  $\sigma_2$  also denoting by  $s$  the diagram that is a permutation of the wires according to  $s$ . We consider the following diagram, where for

each  $k \in \{1, \dots, r'\}$ ,  $C'_k : \top^{\oplus m_k} \rightarrow \top^{\oplus m_k}$  is of the form , and for each  $p \in [n]$ , the  $\text{--}(\star)\text{--}$  on wire  $p$  is  $\text{--}(\star)\text{--}$  if  $\tilde{e}_p$  and  $\tilde{e}_p$  have the same direction, or  $\text{--}(\circ)\text{--}$  otherwise:



For any  $k \in \{1, \dots, r'\}$  and  $\ell \in [m_k]$ , if  $\tilde{e}_p$  and  $\tilde{e}_p$  have the same direction then one has  $\llbracket C_{w, \tau} \rrbracket (\mathbf{V}, i_\ell^k) = ((\mathbf{V}, i_\ell^k), w_{\tau_1(i_\ell^k)})$  and  $\llbracket C_{w, \tau} \rrbracket (\mathbf{H}, i_\ell^k) = ((\mathbf{H}, i_\ell^k), w_{\tau_1(i_{\ell+1 \bmod m_k}^k)})$ , and if they have opposite directions then one has  $\llbracket C_{w, \tau} \rrbracket (\mathbf{V}, i_\ell^k) = ((\mathbf{V}, i_\ell^k), w_{\tau_1(i_{\ell+1 \bmod m_k}^k)})$  and  $\llbracket C_{w, \tau} \rrbracket (\mathbf{H}, i_\ell^k) = ((\mathbf{H}, i_\ell^k), w_{\tau_1(i_\ell^k)})$ . That is, in any case,  $w_{\mathbf{V}, i_\ell^k}^{C_{w, \tau}}$  is the tail of  $\tilde{e}_{i_\ell^k}$  and  $w_{\mathbf{H}, i_\ell^k}^{C_{w, \tau}}$  is its head. Since the indices  $i_\ell^k$  span  $[n]$  entirely, this implies that  $C_{w, \tau}$  has the same semantics as  $C_{w, \sigma}^{\text{opt}, \mathcal{A}'}$ . But  $C_{w, \tau}$  contains  $n - r'$  PBS whereas  $C_{w, \sigma}^{\text{opt}, \mathcal{A}'}$  contains  $n - r$  PBS, so that  $C_{w, \tau}$  contains strictly fewer PBS than  $C_{w, \sigma}^{\text{opt}, \mathcal{A}'}$ , which contradicts the query-PBS-optimality of  $C_{w, \sigma}^{\text{opt}, \mathcal{A}'}$ .



This proves that the edge-partition of  $\tilde{G}$  into cycles obtained from  $C_{w,\sigma}^{\text{opt},\neq}$  has maximum number of cycles among all possible choices of orientation and partition. In other words, the undirected edge-partition of  $G$  obtained by erasing the directions of the edges in this edge-partition of  $\tilde{G}$  has maximum number of cycles. This finishes the reduction.

### A.9.2 Proof of Corollary 33

We reduce this problem from the problem maxDCD of, given an Eulerian directed graph  $\vec{G}$ , finding a maximum-cardinality edge-partition of  $\vec{G}$  into directed cycles. This problem is defined and proved to be NP-hard in [3].

The proof has the same structure as the proof of Theorem 32 : we define  $C_{w,\sigma}$  in the same way, and we consider an equivalent diagram  $C_{w,\sigma}^{\text{opt}}$  which is now query-PBS-optimal only among negation-free diagrams. Since the PGT procedure preserves the property of being negation-free, we can still assume that it is in PGT form. With the same arguments as in the proof of Theorem 32, we can do the same deformations and define  $C_{w,\sigma}^{\text{opt}'}$  in the same way. This time,  $C_{w,\sigma}^{\text{opt}'}$  is negation-free, so that  $C_{w,\sigma}^{\text{opt},\neq} = C_{w,\sigma}^{\text{opt}'}$  and  $\tilde{G} = \vec{G}$ , so the construction of the proof of Theorem 32 gives us an edge-partition of  $\vec{G}$ . To prove that this edge-partition has maximum cardinality, we only have to prove that there is no edge-partition of  $\vec{G}$  into strictly more cycles, and the proof of this is the same as for Theorem 32 (with the difference that we necessarily have  $\tilde{G} = \vec{G}$ , which allows for many simplifications).

### A.9.3 Proof of Corollary 34

The proof relies on the following lemma:

► **Lemma 41.** *Given any diagram  $D$  of  $\mathcal{P}$  which is query-optimal and contains at least one negation, there exists an equivalent negation-free diagram with the same gates containing at most  $\#_{\text{PBS}}(D) + \#_{-}(D) - 1$  PBS.*

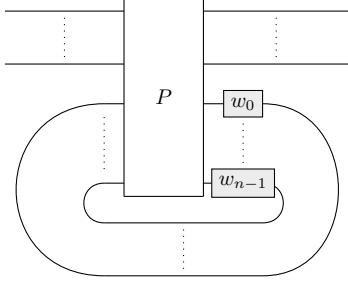
**Proof of Corollary 34.** Note that the proofs of Theorem 32 and Corollary 33 actually give us slightly stronger results than the exact statements of Theorem 32 and Corollary 33, since they in fact consider the restricted versions of their respective problems in which the input diagram is required to be in  $\mathcal{P}$ .

Given Lemma 41, Corollary 34 follows from this stronger version of Corollary 33. Indeed, it suffices to prove that the problem of optimising  $\#_{\text{PBS}}(D) + \alpha\#_{-}(D)$  together with the queries is already NP-hard when restricted to the case where the input diagram  $D$  is negation-free and in  $\mathcal{P}$ . Given such a diagram  $D$ , any query-optimal diagram  $D'$  equivalent to  $D$  such that  $\#_{\text{PBS}}(D') + \alpha\#_{-}(D')$  is minimal, is negation-free. Indeed, if it was not, then, since it is in  $\mathcal{P}$ , by Lemma 41 there would exist an equivalent query-optimal, negation-free diagram  $D''$  that would satisfy  $\#_{\text{PBS}}(D'') + \alpha\#_{-}(D'') = \#_{\text{PBS}}(D'') \leq \#_{\text{PBS}}(D') + \#_{-}(D') - 1 < \#_{\text{PBS}}(D') + \alpha\#_{-}(D')$ , which would contradict the fact that  $\#_{\text{PBS}}(D') + \alpha\#_{-}(D')$  is minimal. Thus, finding a query-optimal diagram  $D'$  equivalent to  $D$  such that  $\#_{\text{PBS}}(D') + \alpha\#_{-}(D')$  is minimal, amounts to finding a diagram equivalent to  $D$  and query-PBS-optimal among negation free diagrams. ◀

It remains to prove Lemma 41:

**Proof of Lemma 41.** Let  $D : \top^{\oplus n} \rightarrow \top^{\oplus n}$  be a query-optimal diagram of  $\mathcal{P}$  containing at least one negation. Let us first apply Step 1 of the PGT procedure, that is, by mere

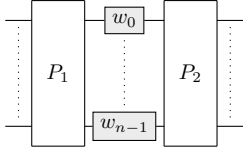
deformation, we put  $D$  in the form



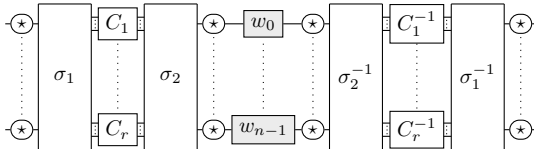
with  $P$  gate-free. Let  $f(P)$  be the number of positions  $p$  such that  $c_{\mathbf{V},p}^P = \mathbf{H}$  (note that this number does not depend on the way of deforming  $D$ ). Since the semantics of  $P$  applies a permutation to the couples  $(c, p)$ , there are the same number of positions  $p$  such that  $c_{\mathbf{H},p}^P = \mathbf{V}$ , so that there are  $2f(P)$  couples  $(c, p)$  such that  $c_{c,p}^D \neq c$ . Each photon that enters  $P$  with a basis state corresponding to one of these couples gets its polarisation changed while traversing  $P$ , which means that it traverses at least one negation. Since each negation can be reached from at most two basis states, this implies that  $f(P) \leq \#_{\neg}(D)$ .

Note that additionally, due to the semantics of  $D$  (since it is in  $\mathcal{P}$ ), for any  $c, c' \in \{\mathbf{V}, \mathbf{H}\}$  and  $p, p' \in [2n]$  such that  $\llbracket P \rrbracket(c, p) = (c', p')$ , one has  $p \in [n]$  if and only if  $p' \in \{n, \dots, 2n-1\}$  and vice-versa, and  $\llbracket P \rrbracket(c', p') = (c, p)$ . Combined with the fact that  $\llbracket P \rrbracket$  applies a permutation to the couples  $(c, p)$ , this implies that there are the same number of positions  $p$  such that respectively:  $p \in [n]$  and  $c_{\mathbf{V},p}^P = \mathbf{H}$ ;  $p \in [n]$  and  $c_{\mathbf{H},p}^P = \mathbf{V}$ ;  $p \in \{n, \dots, 2n-1\}$  and  $c_{\mathbf{V},p}^P = \mathbf{H}$ ;  $p \in \{n, \dots, 2n-1\}$  and  $c_{\mathbf{H},p}^P = \mathbf{V}$ . Since the sum of these four numbers of positions is equal to  $2f(P)$ , this implies that  $f(P)$  is even and that the number of positions  $p$  is equal to  $\frac{f(P)}{2}$  in each case.

By applying the rest of the PGT procedure, we put  $P$  in stair form and thereby transform  $D$  into a diagram  $D'$  in PGT form. With a similar argument as in the proof of Theorem 32, we can put  $D'$  in the form

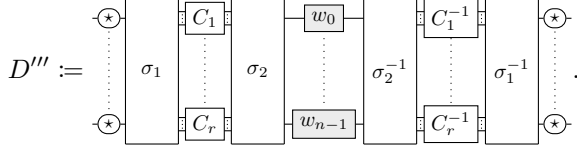


where  $P_1$  and  $P_2$  are in stair form. Since  $D \in \mathcal{P}$ , for any  $c, c' \in \{\mathbf{V}, \mathbf{H}\}$  and  $p, p' \in [n]$ , if  $\llbracket P_1 \rrbracket(c, p) = ((c', p'), \epsilon)$  then  $\llbracket P_2 \rrbracket(c', p') = ((c, p), \epsilon)$ . Hence,  $P_1$  has the same semantics as the horizontal reflection of  $P_2$  and vice-versa. By Theorem 27, this implies that  $P_1$  and  $P_2$  contain the same number of PBS. Therefore, by replacing  $P_2$  by the horizontal reflection of  $P_1$ , we get a diagram  $D''$  which is still equivalent to  $D$  and still has at most as many PBS as  $D$ . As in the proof of Theorem 32, we can write  $D''$  in the form

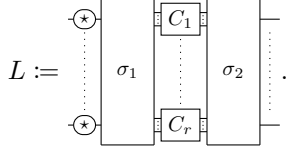


where  $\sigma_1$  and  $\sigma_2$  are permutation of the wires, the  $C_k$  are staircases (see Definition 25), and given any gate-free diagram  $E$ ,  $E^{-1}$  denotes its horizontal reflection. Since  $D''$  is symmetric,

we can remove the negations in the middle without changing its semantics, which gives us



Let

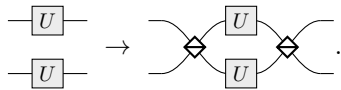


For every letter  $U \in \{w_0, \dots, w_{n-1}\}$ , let  $d_U(D)$  be the number of positions  $p$  such that for some  $p_1, p_2$ , one has  $p_{\mathbf{V}, p_1}^L = p_{\mathbf{V}, p_2}^L = p$  and  $w_p = U$ . Since  $D \in \mathcal{P}$ ,  $U$  appears as many times among the  $w_{\mathbf{V}, p}^D$  as among the  $w_{\mathbf{H}, p}^D$ . Since  $\forall c, p, w_{c, p}^D = w_{p_{c, p}^L}$ , this implies that the number of positions  $p'$  such that for some  $p'_1, p'_2$  one has  $p_{\mathbf{H}, p'_1}^L = p_{\mathbf{H}, p'_2}^L = p'$  and  $w_{p'} = U$  is also  $d_U(D)$ . We arbitrarily associate a position  $p'$  of the second kind with each position  $p$  of the first kind, so as to distribute these  $2d_U(D)$  positions into  $d_U(D)$  couples  $(p, p')$ . By doing so for every  $U \in \{w_0, \dots, w_{n-1}\}$ , we obtain  $d(D)$  couples, where  $d(D) := \sum_{U \in \{w_0, \dots, w_{n-1}\}} d_U(D)$ , with the

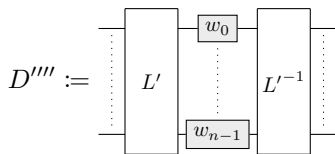
property that every position  $q$  satisfying for some  $p_1, p_2, c, p_{c, p_1}^L = p_{c, p_2}^L = q$ , appears exactly once among these couples (as a left element if  $c = \mathbf{V}$ , and as a right element if  $c = \mathbf{H}$ ).

For each position  $q$  among these  $2d(D)$  positions, there is exactly one polarisation  $c$  such that  $c_{c, p}^L \neq c$ . This property is not affected by appending negations at the right of  $L$ , so that there is also exactly one polarisation  $c$  (for each  $q$ ) such that  $c_{c, q}^{P_1} \neq c$ . By definition of  $P_1$ , there is also exactly one polarisation  $c$  such that  $c_{c, q}^P \neq c$ . Since all of these  $2d(D)$  positions  $q$  are in  $[n]$ , this implies that  $2 \frac{f(P)}{2} \geq 2d(D)$ . Since  $f(P) \leq \#_{-}(D)$ , this inequality implies that  $2d(D) \leq \#_{-}(D)$ .

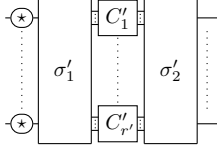
For each of the  $d(D)$  couples  $(p, p')$ , we do the following transformation in  $D'''$  (up to deformation):



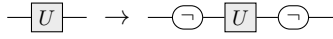
Each time, we put  $L$  in stair form again, we transform  $L^{-1}$  symmetrically so that it remains the horizontal reflection of  $L$ , and we remove any negations at the right of  $L$  and at the left of  $L^{-1}$ , which is possible because  $D'''$  remains symmetric. One can check that if the PBS appended to  $L$  is connected to two different  $C_i$ s, then this results in merging them together, so that the number of PBS stays the same (after adding the additional PBS), and if it is connected to a single  $C_i$  then this results in splitting it into two staircases, so that the number of PBS in  $L$  decreases by 2. The behaviour of  $L^{-1}$  is symmetric. At the end, the total number of PBS is at most  $\#_{\text{PBS}}(D) + 2d(D)$ , and the equality can be reached only if at every step two  $C_i$ s have been merged. This gives us a diagram



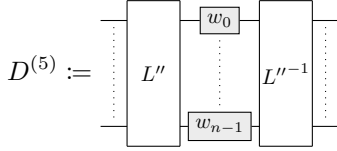
with  $L'$  of the form



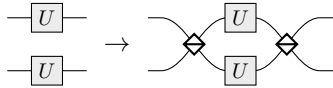
in which there are no couples of positions  $p_1, p_2$  such that  $p_{\mathbf{V}, p_1}^L = p_{\mathbf{V}, p_2}^L$  anymore. In particular, for each position  $p$  such that for some  $p_1$ ,  $\llbracket L' \rrbracket (\mathbf{V}, p_1) = ((\mathbf{H}, p), \epsilon)$ , there exists  $p_2$  such that  $\llbracket L' \rrbracket (\mathbf{H}, p_2) = ((\mathbf{V}, p), \epsilon)$ . For each of these positions, we apply the following transformation:



This gives us a diagram



with  $L''$  such that for all  $c, p$ ,  $c_{c,p}^{L''} = c$ . By putting  $L''$  in normal form, then in stair form again, we get a diagram  $L'''$  without negations and with at most as many *PBS* as  $L''$ . In particular, the resulting diagram  $D^{(6)}$  (after proceeding symmetrically in  $L'''^{-1}$ ) contains at most  $\#_{\text{PBS}}(D) + 2d(D)$  *PBS*. If it has strictly fewer *PBS*, or if  $2d(D) < \#_{-}(D)$ , then we have the desired result. If it has exactly  $\#_{\text{PBS}}(D) + 2d(D)$  *PBS* and  $2d(D) = \#_{-}(D)$ , then this means in particular that at each of the steps of the transformation of  $D'''$  into  $D''''$ , two  $C_i$ s have been merged. By hypothesis,  $\#_{-}(D) \geq 1$ , so the fact that  $2d(D) = \#_{-}(D)$  implies that  $d(D) > 0$ . This implies that there has been at least one step in the transformation of  $D'''$  into  $D''''$ , in which two staircases connected to two gates with the same label have been merged. Since these staircases have not been split, there is at least one couple of gates in  $D^{(5)}$  that have the same label and are connected to the same staircase. Then by applying to them the same transformation as before:



and putting  $L'''$  (and  $L'''^{-1}$ ) in stair form again, we get a diagram with  $\#_{\text{PBS}}(D) + \#_{-}(D) - 2$  *PBS* and no negations, which is equivalent to  $D$ .  $\blacktriangleleft$

## B Derivations of Equations (18) to (24)

Note that Equation (18) is a particular case of Equation (2) and that Equation (19) is a particular case of Equation (26). To prove Equation (20), we derive a more general version, analogous to Equations (2) and (26): for any monoid  $M$  and any  $U, V \in M$ ,

$$\text{---} \boxed{U} \text{---} \boxed{V} \text{---} \stackrel{(9)(5)}{=} \text{---} \begin{array}{c} \text{---} \boxed{U} \text{---} \boxed{V} \text{---} \\ \text{---} \boxed{U} \text{---} \boxed{V} \text{---} \end{array} \text{---}$$

$$\begin{aligned}
 & \stackrel{(2)(26)}{=} \text{Diagram with two diamond nodes and two } VU \text{ boxes} \\
 & \stackrel{(5)(9)}{=} \boxed{VU}
 \end{aligned}$$

To prove Equation (21), we have:

$$\begin{aligned}
 & \begin{array}{c} \mathbf{v} \\ \mathbf{h} \end{array} \boxed{U} \stackrel{(10)}{=} \text{Diagram with two diamond nodes and two } U \text{ boxes} \\
 & \stackrel{(5)}{=} \text{Diagram with two diamond nodes and one } U \text{ box}
 \end{aligned}$$

To prove Equation (22), we have:

$$\begin{aligned}
 & \begin{array}{c} \mathbf{h} \\ \mathbf{v} \end{array} \boxed{U} \stackrel{(21)}{=} \text{Diagram with two diamond nodes and two } U \text{ boxes} \\
 & \stackrel{(11)(12)}{=} \text{Diagram with two diamond nodes and one } U \text{ box}
 \end{aligned}$$

To prove Equation (23), we have:

$$\begin{aligned}
 & \begin{array}{c} \mathbf{v} \\ \mathbf{v} \end{array} \boxed{U} \stackrel{(7)(3)}{=} \begin{array}{c} \mathbf{v} \\ \mathbf{v} \ominus \end{array} \boxed{U} \ominus \\
 & \stackrel{(21)}{=} \text{Diagram with two diamond nodes and one } U \text{ box}
 \end{aligned}$$

To prove Equation (24), we have:

$$\begin{aligned}
 & \begin{array}{c} \mathbf{h} \\ \mathbf{h} \end{array} \boxed{U} \stackrel{(8)(3)}{=} \begin{array}{c} \mathbf{h} \ominus \\ \mathbf{h} \end{array} \boxed{U} \ominus \\
 & \stackrel{(21)}{=} \text{Diagram with two diamond nodes and one } U \text{ box}
 \end{aligned}$$



**C PGT Procedure**

**C.1 Full Description of the Procedure**

0. During the whole procedure, every time there are two consecutive negations, we remove them using Equation (7), (8) or their all-black version:

$$\neg\neg = \text{---} \tag{28}$$

1. Deform  $D_0$  to put it in the form (A) with  $P$  gate-free. The goal of the following steps is to put  $P$  in stair form.
2. Split all PBS of the form  $\begin{matrix} a \\ b \end{matrix} \diamond$  into combinations of  $\begin{matrix} \text{---} \\ \text{---} \end{matrix} \diamond$ ,  $\begin{matrix} \text{---} \\ \text{---} \end{matrix} \diamond$  and  $\begin{matrix} \text{---} \\ \text{---} \end{matrix} \diamond$ , using Equations (13) to (17).
3. As long as there are two PBS connected by a black wire, with possibly a black negation on this wire, push this negation out (if present) using Equation (4), and cancel the PBS together using Equation (10). It may be necessary to flip the PBS upside down using Equation (11) and/or (12) in order to be able to apply Equations (4) and (10). Note also that to cancel the two PBS together one may have to use dinaturality:

When there are not two such PBS anymore, all black wires are connected to at least one side of  $P$  (possibly through negations), and the PBS are connected together with red and blue wires with possibly negations on them.

4. Remove all loops using the following equations:

$$\text{red loop} \text{ v} = \text{---} \tag{29}$$

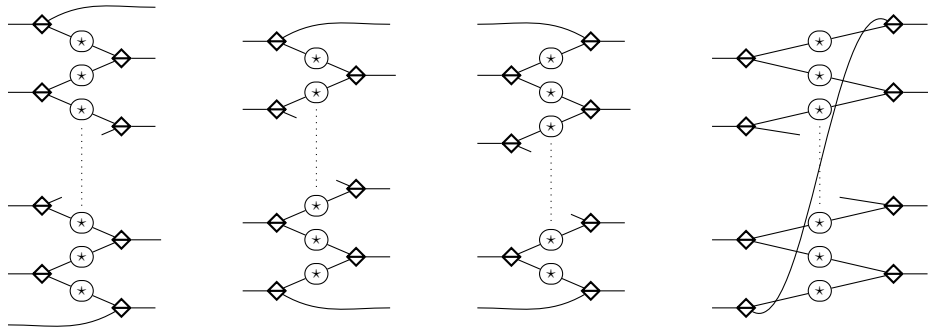
$$\text{blue loop} \text{ h} = \text{---} \tag{30}$$

$$\text{black loop} = \text{---} \tag{31}$$

$$\text{black loop with negation} = \text{---} \tag{32}$$

Note that since  $D_0$  is query-optimal, there cannot be loops containing gates at this point.

5. Deform  $P$  to put it in the form (B) with  $\sigma_1$  and  $\sigma_2$  being wire permutations and the  $C_i$  being trace-free and connected. It remains to transform the  $C_i$  into staircases. Up to additional deformation of  $P$  in order to reorder the input and output wires of the  $C_i$ , and to using Equations (11) and (12), every  $C_i$  is of one of the following forms:



where  $\neg(\star)$  is either  $\frac{a}{\neg}$  or  $\frac{a}{\neg}\neg$  with  $a \in \{v, h\}$ ,  $\neg\langle \diamond \rangle$  is either  $\neg\langle \diamond \rangle$  or  $\langle \diamond \rangle\neg$  and  $\langle \diamond \rangle$  is either  $\langle \diamond \rangle$  or  $\langle \diamond \rangle$ .

- Remove the negations in the middle of the  $C_i$  by pushing them to the bottom by means of Equation (4) and its following variants (all of the form “a three-wire PBS with a negation on one of the three wires is equal to this PBS reflected vertically with negations on the other two wires”; note that Equations (4), (33), (34) and (35) have to be applied from right to left, while Equations (36), (37), (38) and (39) have to be applied from left to right):

$$\neg\langle \diamond \rangle = \langle \diamond \rangle\neg\neg \quad (33)$$

$$\langle \diamond \rangle\neg = \neg\langle \diamond \rangle\neg \quad (34)$$

$$\langle \diamond \rangle = \neg\langle \diamond \rangle\neg \quad (35)$$

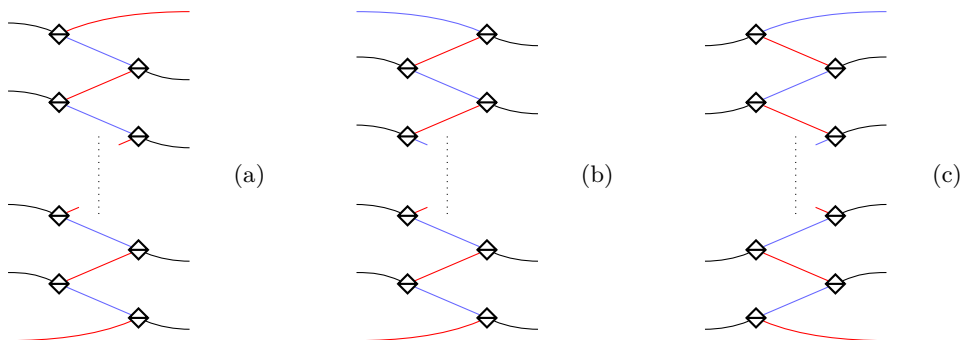
$$\langle \diamond \rangle\neg = \langle \diamond \rangle\neg\neg \quad (36)$$

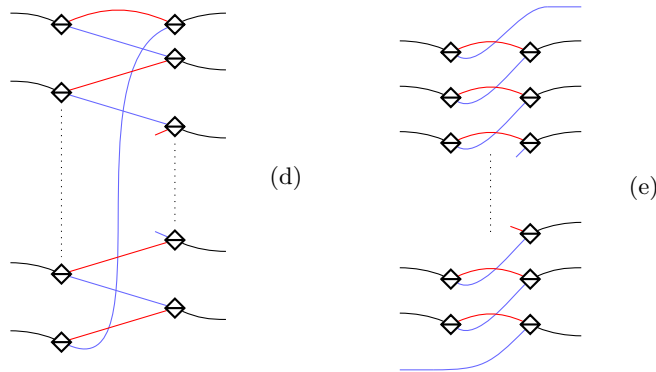
$$\langle \diamond \rangle = \langle \diamond \rangle\neg\neg \quad (37)$$

$$\neg\langle \diamond \rangle = \neg\langle \diamond \rangle\neg \quad (38)$$

$$\langle \diamond \rangle\neg = \langle \diamond \rangle\neg\neg \quad (39)$$

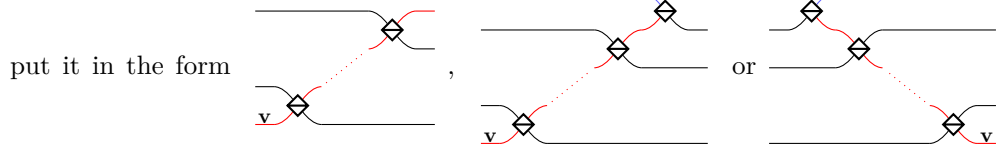
- Up to deforming  $P$  in order to flip the  $C_i$  upside down, and to using Equations (11) and (12) wherever necessary, every  $C_i$  is now of one of the following forms (note that it is easy to know of which form each  $C_i$  should be, before deforming it, by looking at its input/output type):





Transform each of them into one of the five kind of staircases depicted in Definition 25, depending on its type:

- If  $C_i$  is of the form (a), (b) or (c), then repeatedly apply Equation (14) or (15) to

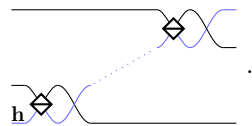


respectively.

- If  $C_i$  is of the form (e), then repeatedly apply the following equation:

$$\text{Diagram} = \text{Diagram} \tag{40}$$

to put it in the form



- If  $C_i$  is of the form (d), then repeatedly apply the following variant of Equation (10):

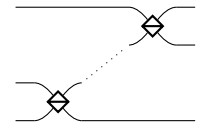
$$\text{Diagram} = \text{Diagram} \tag{41}$$

and Equation (13), as follows:

$$\text{Diagram} \stackrel{(41)}{=} \text{Diagram} \stackrel{(13)}{=} \text{Diagram} \tag{13}$$



and finally apply Equation (9) once, in order to put it in the form

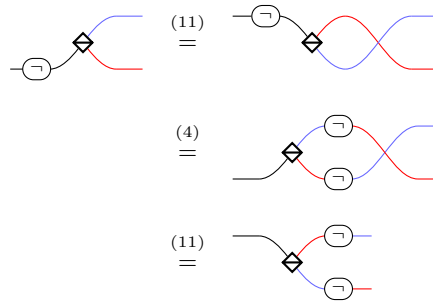


This gives us the desired diagram  $D_1$  and finishes the procedure.

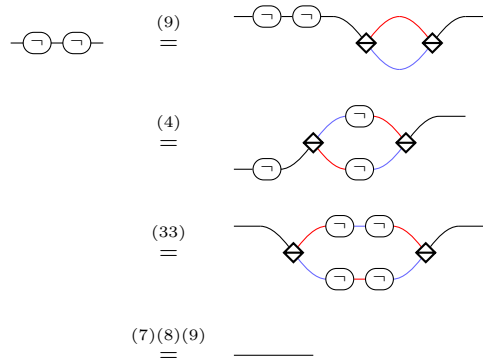
### C.2 Derivations of the Ancillary Equations

We have to derive Equations (28) to (41) from the equations of Figure 4. In order to benefit from some dependencies between the derivations, we treat the equations in the following order: (33), (28), (29), (30), (31), (41), (32), (34), (35), (36), (37), (38), (39), (40).

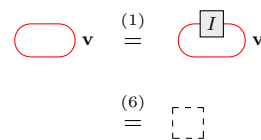
For Equation (33), the derivation is the following:



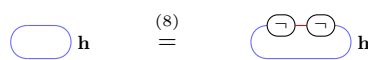
For Equation (28):



For Equation (29):



For Equation (30):



$$\begin{aligned}
 & \stackrel{\text{dinaturality}}{=} \text{[Diagram: A red loop with two small circles containing minus signs, labeled } \mathbf{v} \text{]} \\
 & \stackrel{(7)}{=} \text{[Diagram: A simple red loop, labeled } \mathbf{v} \text{]} \\
 & \stackrel{(29)}{=} \text{[Diagram: A dashed square]}
 \end{aligned}$$

For Equation (31):

$$\begin{aligned}
 & \stackrel{(9)}{=} \text{[Diagram: A black loop with two diamond-shaped nodes, one red and one blue, connected by arcs]} \\
 & \stackrel{\text{dinaturality}}{=} \text{[Diagram: A red loop with two diamond-shaped nodes, one red and one blue, connected by arcs]} \\
 & \stackrel{(10)}{=} \text{[Diagram: A blue loop with two diamond-shaped nodes, one red and one blue, connected by arcs, labeled } \mathbf{h} \text{]} \\
 & \stackrel{(30)(29)}{=} \text{[Diagram: A dashed square]}
 \end{aligned}$$

For Equation (41):

$$\begin{aligned}
 & \stackrel{(11)}{=} \text{[Diagram: A crossing of red and blue lines with two diamond-shaped nodes]} \\
 & \stackrel{(10)}{=} \text{[Diagram: A crossing of red and blue lines with labels } \mathbf{v} \text{ and } \mathbf{h} \text{]}
 \end{aligned}$$

For Equation (32):

$$\begin{aligned}
 & \stackrel{(9)}{=} \text{[Diagram: A black loop with two diamond-shaped nodes and a small circle with a minus sign]} \\
 & \stackrel{(4)}{=} \text{[Diagram: A black loop with two diamond-shaped nodes and two small circles with minus signs]} \\
 & \stackrel{\text{dinaturality}}{=} \text{[Diagram: A complex loop with two diamond-shaped nodes, two small circles with minus signs, and red and blue arcs]} \\
 & \stackrel{(41)}{=} \text{[Diagram: A complex loop with two diamond-shaped nodes, two small circles with minus signs, and red and blue arcs, labeled } \mathbf{h} \text{ and } \mathbf{v} \text{]}
 \end{aligned}$$

$$\begin{aligned}
 &= \text{Diagram with two circles containing } \neg \text{ and } \neg \text{ connected by a blue line, labeled } h \\
 &\stackrel{(8)(31)}{=} \text{Diagram with a dashed square}
 \end{aligned}$$

For Equation (34):

$$\begin{aligned}
 &\text{Diagram with a diamond and a circle containing } \neg \text{ on a red line} \stackrel{(9)}{=} \text{Diagram with two diamonds and a circle containing } \neg \text{ on a red line} \\
 &\stackrel{(4)}{=} \text{Diagram with two diamonds and two circles containing } \neg \text{ on a red line} \\
 &\stackrel{(41)}{=} \text{Diagram with two diamonds and two circles containing } \neg \text{ on a red line} \\
 &\stackrel{(12)}{=} \text{Diagram with two diamonds and two circles containing } \neg \text{ on a red line}
 \end{aligned}$$

For Equation (35):

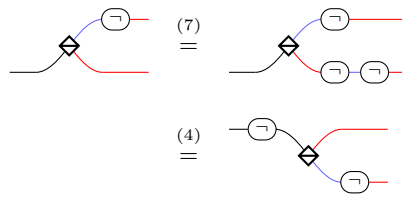
$$\begin{aligned}
 &\text{Diagram with a diamond and a circle containing } \neg \text{ on a red line} = \text{Diagram with two diamonds and a circle containing } \neg \text{ on a red line} \\
 &\stackrel{(12)}{=} \text{Diagram with two diamonds and a circle containing } \neg \text{ on a red line} \\
 &\stackrel{(34)}{=} \text{Diagram with two diamonds and two circles containing } \neg \text{ on a red line} \\
 &\stackrel{(12)}{=} \text{Diagram with two diamonds and two circles containing } \neg \text{ on a red line}
 \end{aligned}$$

For Equation (36):

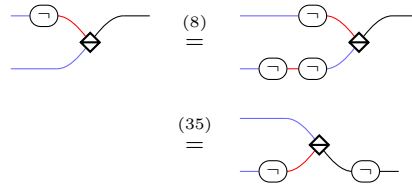
$$\begin{aligned}
 &\text{Diagram with a diamond and a circle containing } \neg \text{ on a red line} \stackrel{(8)}{=} \text{Diagram with two diamonds and two circles containing } \neg \text{ on a red line} \\
 &\stackrel{(33)}{=} \text{Diagram with two diamonds and two circles containing } \neg \text{ on a red line}
 \end{aligned}$$

For Equation (37):

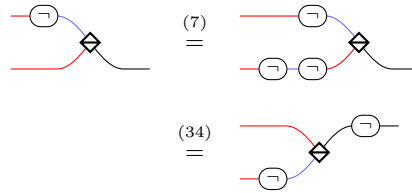




For Equation (38):



For Equation (39):



For Equation (40):

